

FLUID MECHANICS OF PROPULSION BY CILIA AND FLAGELLA

✱8107

Christopher Brennen and Howard Winet

Division of Engineering and Applied Science, California Institute of Technology,
Pasadena, California 91125

1 INTRODUCTION

1.1 *Opening Remarks*

Since the *Annual Review of Fluid Mechanics* first published a review on micro-organism locomotion by Jahn & Votta (1972) considerable progress has been made in the understanding of both the biological and the fluid-mechanical processes involved not only in microorganism locomotion but also in other fluid systems utilizing cilia. Much of this knowledge and research, which has been built on the solid foundation of the pioneering work of Sir James Gray (1928, 1968) and Sir Geoffrey Taylor (1951, 1952a,b), has been reported extensively elsewhere, particularly by Gray (1928, 1968), Sleigh (1962), Lighthill (1975), and Wu, Brokaw & Brennen (1975). The subject is now sufficiently broad that it precludes any exhaustive treatment in these few pages. Rather, we restrict this review primarily to a summary of present understanding of the low-Reynolds-number flows associated with micro-organism propulsion and the hydromechanics of ciliary systems. In this introductory section we wish to put such fluid-mechanical studies in biological perspective. Section 2 outlines the present status of low-Reynolds-number slender-body theory, and we discuss the application of this theory to biological systems in the final sections.

1.2 *Ciliary and Flagellar Propulsion in Perspective*

In the scheme of life the role of contractile elements is a major one. Some life functions are totally dependent on them and others are more efficient because of them. When considered as isolated structures, contractile elements are those that use up biochemical energy in doing mechanical work. But the artificiality of such isolation becomes evident when one considers the role of contractility in the two other kinds of work requiring biochemical energy, synthesis and concentration (Lehninger 1971). Consider, for example, the process by which bone is aided in its growth by motion-generated stresses (Black & Korostoff 1974). By such relationships

contractility contributes significantly to biosynthesis. Consider also the recent demonstration that cilia lining the brain ventricles have a significant effect on transmural transport in the ependyma (Nelson 1975), and the link between contractility and concentration will be established. To be sure, concentration and biosynthesis can be said to generate some movements; the most familiar examples are the growth tropisms (geo- and photo-) and the opening and closing of stomates caused by turgor pressure changes, which is characteristic of the higher vascular plants. This review is not, however, concerned with noncontractile adaptations. In any case, it is a gross oversimplification to view contractile structures as isolated elements for they are an integral part of the life functions to which they contribute.

Contractile elements can be grouped into four classes for convenience: 1. prokaryotic flagella, 2. cytoplasmic filaments or microtubules, 3. eukaryotic cilia and flagella, and 4. smooth or striated muscle. Although only the first and third classes are the concern of this review, some perspective into the utility of each type of contractile element can be gained by an all-inclusive overview such as the one presented in Table 1. This table illustrates how natural selection has distributed the mechanisms of contractility among living things and their life functions. The life functions that directly include some aspect of propulsion are irritability, contractility, ingestion, digestion, circulation, reproduction, respiration, and excretion.

It may also be noted upon examination of the table that no mode of contraction has gained the exclusive right to serve a given life function. This diversity has come about not only because natural selection is opportunistic (i.e. whichever adaptation works at the "moment of truth" is the one selected for) but also because at least two classes of contractile elements—cytoplasmic microtubules and eukaryotic flagella—are interchangeable (e.g. the amoebflagellate *Naegleria*).

In order for contractile elements to maintain required services for the life functions they attend and in order for them to assist in biosynthetic and concentration work, they must be provided with biochemical energy and structural replacements by biosynthesis (which includes chemical respiration) and concentration. Such interdependence is a natural consequence of the division of labor that is so characteristic of living systems and that must be kept in mind lest one be tempted to analyze *in situ* contraction as an isolated process. Inversely, this interdependence has the benefit of allowing one to learn some of the details about biosynthesis and concentration from their contributions to the contractile process.

In general the elucidation of propulsion by contractile elements is just as much an exercise in relating structure and function as is any other biological investigation. By contractile structure we mean the somewhat stable part of the contractile element—the components that actually move—while function refers to the motion, which is to say the performance of mechanical work. Such a division is, of course, artificial not only because changes in structure accompany all contractions (e.g. cytoplasmic streaming in amoebas) but also because the propulsive structure of the system—i.e. the part of the contractile system in contact with the fluid—and the physical structure of the fluid—density, homogeneity, viscosity, pressure, etc.—interact to form a dynamic feedback relationship that is not always predictable from knowledge of structure alone.

Table 1 The occurrence of contractile elements in organism life functions^a

Biological group	Locomotion	Ingestion	Digestion	Irritability	Circulation	Reproduction	Respiration	Excretion
Prokaryotes								
EUBACTERIA	flagellum			flagellum?		flagellum		
SPIROCHAETIS	flagellum(?)			flagellum?		cytoplasm		
BLUE-GREEN ALGAE	flagellum				cytoplasm	flagella		
Vascular Plants	-							
Protista								
FLAGELLATA	flagellum	flagellum	cytoplasm	flagellum?	cytoplasm	flagellum		cytoplasm
AMOEBA	cytoplasm	cytoplasm	cytoplasm	cytoplasm?	cytoplasm	cytoplasm		cytoplasm
CILIATA	flagellum	cilia	cytoplasm	cytoplasm?	cytoplasm	flagella		cytoplasm
	cytoplasm					cytoplasm		
(spasmoneme)						cilia		
Animals								
PORIFERA	flagella (larvae)	flagella	cytoplasm		flagella	cytoplasm	flagella	flagella
	striated muscle	smooth muscle	cytoplasm			flagella		
Cnidaria	smooth muscle	striated muscle	cilia	cilia (in ctenophores)	cilia	flagella	cilia	cilia
	cilia (larvae)	cytoplasm				cilia		
PLATYHELMINTHIA	smooth muscle	smooth muscle	smooth muscle	cilia	-	smooth muscle		cilia
	cilia		cytoplasm			flagella		
NEMATODA	smooth muscle	smooth muscle	smooth muscle			cytoplasm		
	smooth muscle		smooth muscle			cytoplasm		
ANNELIDA	smooth muscle	smooth muscle	smooth muscle	cilia	cilia (where blood system absent)	smooth muscle	smooth muscle	cilia
	cilia (larvae)	cilia	striated muscle		smooth muscle	flagella		smooth muscle
ARTHIPODA	striated muscle	smooth muscle	striated muscle	striated muscle	striated muscle	smooth muscle	striated muscle (invertebrates)	cilia (few species)
	smooth muscle	striated muscle	striated muscle	(which moves sensory organs)	striated muscle	smooth muscle	smooth muscle	striated muscle
				smooth muscle (chromophores)?	smooth muscle	flagella	smooth muscle	cilia
MOLLUSCA	striated muscle	striated muscle	cytoplasm		smooth muscle	flagella	striated muscle	cytoplasm
	smooth muscle	cilia	cilia		striated muscle	flagella	cilia (gills)	
	cilia (larvae)	cilia	smooth muscle	cilia (larvae)		flagella		cytoplasm
ECTOPROCTA	cilia	cilia	cilia			flagella		
	striated muscle	striated muscle	cytoplasm		cilia	flagella, cilia	cilia	cytoplasm
ECHINODERMATA	striated muscle	striated muscle	cilia			cytoplasm		
	smooth muscle	smooth muscle	smooth muscle		smooth muscle	smooth muscle		
	cilia (larvae)		smooth muscle		cardiac muscle	smooth muscle		smooth muscle
CHORDATA (vertebrates only)	striated muscle	striated muscle	smooth muscle	cilia (in membrane lining ventricles)	smooth muscle	flagella	cilia	smooth muscle
	cytoplasm (of fibroblasts, white blood cells, etc)	cilia (in groups below reptiles)	cilia (in groups below reptiles)	(e.g. ciliary muscle)	striated muscle	striated muscle	striated muscle	cilia (in groups below birds)

^a Compiled from Andrew (1959), Barber (1974), Bharier & Rittenberg (1971), Borradaile & Potts (1958), Bourne (1960), Gardner (1976), Prosser (1973), Rivera (1962), Smith et al (1971), and Weiss-Fogh (1975).

1.3 *An Overview of Structure and Function of Whiplike Contractile Elements*

The contractile elements considered in this review are all slender oscillators that are responsible for propulsion of the organism in the fluid or propulsion of the fluid alone. They are called *cilia* or *flagella*, but the latter term is somewhat ambiguous because it is used for two evolutionarily unrelated structures: prokaryotic and eukaryotic flagella. Furthermore, cilia and eukaryotic flagella are closely related organelles having essentially the same structure (Section 5.1) for a given motion, and both utilize ATP as a primary energy source. The energy source for prokaryote motility is unknown (Larsen et al 1974), however, so there are few restrictions at present on the energy aspects of models for their motion. What can be said with some conviction is that this energy is devoted to helping the microbe move to a new environment, an ability that gives the motile prokaryote a distinct advantage over the nonmotile one.

2 FLUID MECHANICS OF SLENDER BODIES AT LOW REYNOLDS NUMBERS

2.1 *Background*

Since the oscillatory motions of cilia and flagella produce a mean translational motion it is important to define two Reynolds numbers, one for each kind of motion. The Reynolds number defined by the propulsive velocity, U , and the typical dimension of the organism L is UL/ν where ν is the kinematic viscosity of the organism's liquid environment; values range from 10^{-6} for many bacteria to about 10^{-2} for spermatozoa, and most of the organisms considered here lie within this range. Equally important is an oscillatory Reynolds number, Re , based on the radian frequency of beating of the organelle, ω , and the typical length of that organelle, l ($Re = \omega l^2/\nu$); typical values of this quantity are about 10^{-3} . Thus the fluid motions that result are dominated by viscous forces and the inertial forces usually play little part in the propulsive mechanisms. Of course there exist organisms in all ranges of Reynolds number, but the difficulties in the fluid-mechanical analyses when the Reynolds numbers approach unity are such that little quantitative work has as yet been done for natural swimming in this regime.

Before we can deal sensibly with the hydromechanics of cilia and flagella it is necessary to digress and discuss the fluid-mechanical basis for the analyses of the low-Reynolds-number flows past slender bodies. That we return to these basic principles is a reflection of the fact that the study of these biological systems has actually been one of the principal motivating factors for the development of slender-body theory at low Reynolds numbers (the other being studies of suspensions of elongated particles).

2.2 *Fundamental Singularities*

Analysis of the detailed hydrodynamics of low-Reynolds-number flows due to cilia and flagella has been greatly aided by the development of methods to construct the flow fields by means of distributions of fundamental singularities. For the purpose

of describing these methods we must dwell briefly on the nature of the fundamental solutions to the equations of motion for an incompressible inertialess Newtonian fluid of viscosity μ . They consist of a continuity condition on the fluid velocity \mathbf{u} ,

$$\nabla \cdot \mathbf{u} = 0, \quad (1)$$

and since there are no inertial forces, a condition of force equilibrium

$$\nabla p = \mu \nabla^2 \mathbf{u} \quad (2)$$

containing the fluid pressure, p . From this it follows that p is a harmonic function, and since $\nabla^4 \mathbf{u} = 0$, the velocity is a bi-harmonic function. The primary fundamental solution to these equations due to a single point force, \mathbf{F} , in an unbounded inertialess fluid was first obtained by Oseen (1927), developed further by Burgers (1938), and named a *stokeslet* by Hancock (1953). If one represents the strength and direction of the singular force at the origin of a coordinate system \mathbf{x} by $8\pi\mu\boldsymbol{\alpha}$, where $\boldsymbol{\alpha}$ denotes the stokeslet strength and direction, the resulting fluid velocity and pressure are, respectively, (see, for example, Chwang & Wu 1975)

$$\begin{aligned} \mathbf{u}(\mathbf{x}; \boldsymbol{\alpha}) &= \boldsymbol{\alpha}/r + (\boldsymbol{\alpha} \cdot \mathbf{x})\mathbf{x}/r^3, \\ p(\mathbf{x}; \boldsymbol{\alpha}) &= 2\mu\boldsymbol{\alpha} \cdot \mathbf{x}/r^3, \end{aligned} \quad (3)$$

where $r = |\mathbf{x}|$. It follows that a derivative of any order of this solution is also a solution to the basic equations. Thus one can construct higher-order singularities such as a Stokes doublet, Stokes quadrupole, etc. Batchelor (1970b) indicated how a Stokes doublet could be decomposed into an antisymmetric component representing the flow field due to a singular moment of strength $8\pi\mu\boldsymbol{\gamma}$ and called a *couplet* [Chwang & Wu (1974) call this a *rotlet*] with velocity and pressure

$$\mathbf{u} = \boldsymbol{\gamma} \times \mathbf{x}/r^3; \quad p = 0 \quad (4)$$

and a symmetric component representing a pure straining or extensional motion of the fluid and termed a *stresslet*. Furthermore, a Laplacian of the stokeslet solution leads to a *potential doublet* of strength δ for which

$$\mathbf{u} = -\delta/r^3 + 3(\delta \cdot \mathbf{x})\mathbf{x}/r^5; \quad p = 0 \quad (5)$$

and which has zero vorticity. One sees that this has the same kinematic form as the conventional doublet in potential flow of an inviscid fluid but that its dynamic contribution to pressure is now zero because the inertia terms have been deleted.

Hancock (1953) seems to have been the first to attempt to use linear superposition of these singularities [permissible because the basic Equations (1) and (2) are linear] in order to construct the fluid mechanics of flagellated microorganisms; his classic work with Sir James Gray (Gray & Hancock 1955) remains a landmark in this respect for both biologists and fluid dynamicists. These works are the forerunners of slender-body theory and resistive-force theory as applied to microorganism locomotion; we return to these subjects shortly.

Chwang & Wu (1974, 1975) and Chwang (1975) have recently shown how solutions to many complex flows may be constructed by superposition of these fundamental

singularities; indeed, for mathematically simple bodies such as spheroids in mathematically simple flow fields (uniform flow, shear flow, quadratic flow, extensional flow, etc) exact solutions are obtained. The simplest example is that of rectilinear translation (at velocity U) of a sphere of radius a , which requires at the center of the sphere only a stokeslet of strength $3aU/4$ in the forward direction and a potential doublet of strength $a^3U/4$ in the opposite direction in order to satisfy the no-slip boundary condition at the surface of the sphere. Indeed, one can visualize the stokeslet as simulating the drag on the body; this is the dominating effect in the far-field since a stokeslet, being the lowest-order singularity, decays least rapidly (like $1/r$). Furthermore, the potential doublet provides the finite geometry of the body in the near-field and its velocity contribution is necessary to satisfy the no-slip condition at the body surface (see Lighthill 1975, p. 48).

We reiterate Chwang & Wu's (1975) observation on the exact solution for the translation of a prolate spheroid of major axis, a , and minor axis, b . They observed that if the translational velocity is decomposed into components U_s and U_n parallel and perpendicular to the major axis and if one examined the force on an element of this spheroid contained between two planes perpendicular to the major axis and length ds apart, then this was composed of two components F_s and F_n in the same two directions where

$$F_s = -C_s U_s ds; \quad F_n = -C_n U_n ds, \quad (6)$$

and C_s and C_n were simple constants dependent only on μ , a , and b and independent of the position of the element or the velocities U_s and U_n . This is a remarkable example of a case in which the resistive-force theory that we examine below holds exactly, irrespective of the slenderness of the body. For a slender prolate spheroid such that $b/a = \epsilon \ll 1$, the resistive coefficients, C_s and C_n , become

$$C_s = \frac{2\pi\mu}{\ln(2a/b) - \frac{1}{2}} [1 + O(\epsilon^2)] \quad (7)$$

$$C_n = \frac{4\pi\mu}{\ln(2a/b) + \frac{1}{2}} [1 + O(\epsilon^2)] \quad (8)$$

2.3 Small Inertial Effects

It is wise to note at this point that the solutions above represent exact solutions only at zero Reynolds number. Introduction of the small contribution of inertia at low but finite Reynolds numbers necessitates re-examination of the far-field where the magnitude of the inertia terms becomes comparable with the viscous terms and leads, for example, to the well-known Stokes paradox for translation of an infinitely long cylinder. Linearization of these far-field inertia effects by means of Oseen's approximation still, however, permits the construction of flow fields by means of a modified set of fundamental solutions in which the *oseenlet* replaces the stokeslet. Developments of slender-body theory along these lines is only beginning [see a recent paper by Chwang & Wu (1976)]. Finally it should also be noted that, of course, there exists the fundamental solution of the entire Navier-Stokes equations for a singular force known as the *round laminar jet* and due to Slezkin (1934),

Landau (1944), and Squire (1951). The stokeslet is simply the limiting case of the round laminar jet for an inertialess fluid. However the nonlinearity of the Navier-Stokes equations does *not* permit superposition of these fundamental solutions.

2.4 Image Systems for Singularities

In the proximity of a boundary, whether it is a solid wall, a free surface, or a hypothetical boundary simulating a line of symmetry in the flow under consideration, it becomes advantageous to develop image systems for the fundamental singularities constructed so that the boundary conditions on that wall are automatically satisfied. In inviscid potential flow this is usually a simple matter since, for example, a solid-plane boundary requires only the identical singularity at the image point in order to satisfy the condition of zero normal velocity. At low Reynolds numbers one must also satisfy the no-slip condition, and the types of singularity required at the image point in order to accomplish this are not immediately obvious. Blake (1971c) obtained the image system for a stokeslet (at various orientations) in a stationary plane boundary, and more recently Blake & Chwang (1974) derived similar image systems for a couplet, a source, and a potential doublet. Some of these are indicated schematically in Figure 1. One of the important effects of the presence of the wall (or equivalently the image system) is that the nature of the far-field is altered. A stokeslet oriented parallel to a wall leads to a far-field, which is a stokes doublet

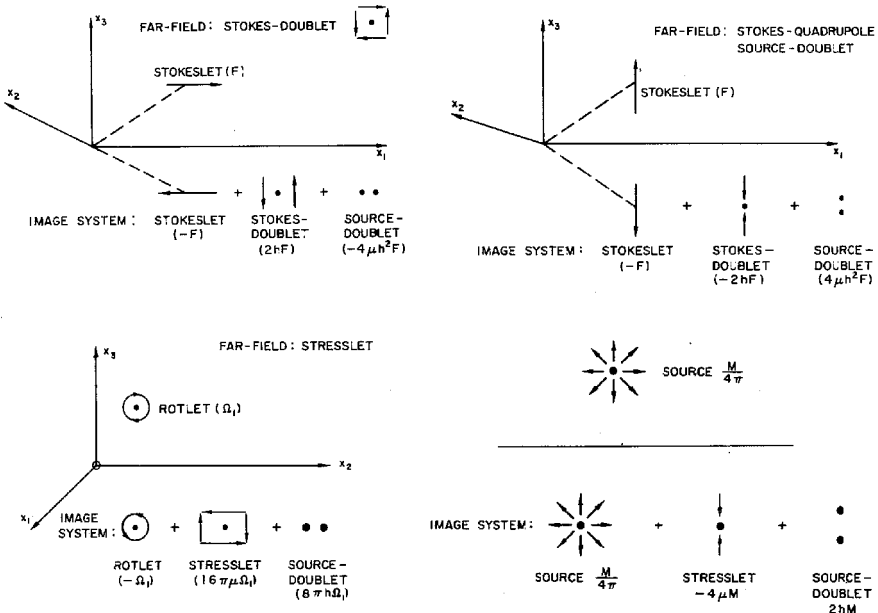


Figure 1 The image singularities in a no-slip boundary (x_1, x_2 plane) for a stokeslet tangential to the boundary, a stokeslet normal to the boundary, a rotlet whose axis is parallel to the boundary, and a source.

decaying like r^{-2} rather than the r^{-1} of a stokeslet in unbounded fluid. On the other hand the far-field of a stokeslet oriented perpendicular to a wall is even weaker and is like a stokes quadrupole or potential doublet. Blake & Sleigh (1974) believe that this has important consequences for the hydromechanics of cilia or for flagella near walls. The far-fields of the other singularities in the presence of a wall are similarly affected, the far-fields for both a rotlet and a source becoming stresslets (like r^{-2}); note that this differs from the far-field of a source near a wall in inviscid potential flow in the absence of a no-slip condition that is like a potential doublet (r^{-3}).

2.5 Slender-Body Theory

The objective of slender-body theory is to take advantage of the slenderness in order to achieve simplifications in obtaining approximate solutions for the flow around such bodies. The development of low-Reynolds-number slender-body theory evolved through the work of Burgers (1938), Broersma (1960), and Tuck (1964); recent work by Taylor (1969), Tillett (1970), Batchelor (1970a), Cox (1970), and Blake (1974b) has concentrated on construction of slender-body solutions by distributions of fundamental singularities along an axis of the body. [With the exception of Batchelor's (1970a) work on arbitrary cross-section, researchers have concentrated on bodies of circular cross-section.] A simple but elegant demonstration of low-Reynolds-number slender-body theory is given by Lighthill (1975, p. 49).

In choosing axes fixed relative to a particular section of the slender body under examination (Figure 2), one seeks the distribution of stokeslets, doublets, etc on the axis of the body that will satisfy the no-slip condition at points such as *A* on the surface of the slender body (local radius is *a*). The integrated induced velocity at such points must then be equated with the known or assumed translational velocity of the section under consideration. The result will, in general, be a system of complicated integral equations for the strength of the singularity distributions. The first simplification of slender-body theory results from the observation that the velocities induced at *A* by singularities outside a certain "near-field" will be dominated by the stokeslets in the "far-field" since their far-field effect (like r^{-1}) dominates that of the other singularities. Thus the primary distribution is one of stokeslets along the entire axis of the body. The boundary condition at the cross-section under consideration is satisfied by introducing a potential doublet (or if necessary other

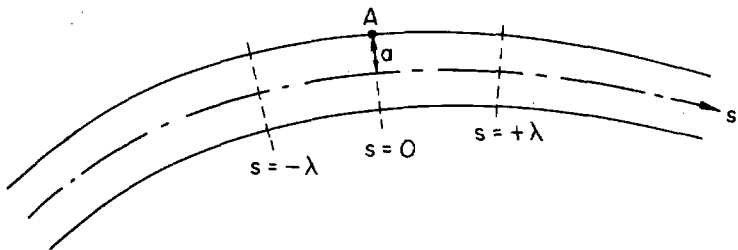


Figure 2 Slender-body schematic.

singularities) only within the near-field. In particular the integrated effect of singularities with a far-field decay faster than r^{-1} can be fairly accurately determined by terminating the integration at some distance $s = \pm\lambda$ from the section under consideration where $s_1, s_2 \gg \lambda \gg a$, s_1 and s_2 being the distances to the ends of the slender body. On the other hand, the integration for the velocity induced by the stokeslets cannot be truncated in this way and indeed yields a velocity with terms like $\ln(s_1 s_2/a^2)$. The reader is referred to Lighthill (1975, p. 49) for the forms of the integrated induced velocities. Note that this is another manifestation of Stokes' paradox for the translation of an infinitely long cylinder; when s_1 or s_2 tend to infinity, the boundary condition at the section under consideration cannot be satisfied. We must also note that such a construction is limited to sections sufficiently far from the ends of the slender body; Tillett (1970) has examined some of the problems associated with such "end effects."

The net result of these considerations is that one must seek the strength and direction of stokeslets distributed along the entire axis of the slender body plus the local distribution of higher-order singularities that satisfies the required boundary condition at every point on the slender-body surface. A useful approximate way of implementing this has been suggested by Lighthill in his John von Neumann lecture (June 1975 at Rensselaer Polytechnic Institute, Troy, New York) and by R. Johnson and T. Y. Wu (private communication). If the local radius of curvature of the body is large compared with a , then the combined effects of both the near- and far-field distributions may be replaced by a distribution of stokeslets alone in the far-field regions, $s > \delta$ and $s < -\delta$. For the components of the stokeslets normal to the axis, $\delta = a/2\sqrt{e}$, whereas for the components tangential to the axis, $\delta = a\sqrt{e}/2$. This observation considerably simplifies the algebra required in obtaining solutions for the motions of slender bodies of more complicated geometry.

The simplest solutions are those for the translation of straight slender cylinders as obtained by Tillett (1970) and Cox (1970). Defining force coefficients as the force per unit length of the body divided by the translational velocity, U , Cox (1970) improved on the original work of Burgers (1938) and Broersma (1960) to show that the force coefficient for a cylinder, with length $2l$ and maximum radius a , moving perpendicular to its axis was

$$C_n = \frac{4\pi\mu}{\ln(2l/a) + C_1} + O\left[\frac{\mu}{(\ln l/a)^3}\right], \quad (9)$$

while that for motion parallel with its axis, C_s , was

$$C_s = \frac{2\pi\mu}{\ln(2l/a) + C_2} + O\left[\frac{\mu}{(\ln l/a)^3}\right]. \quad (10)$$

The value of C_2 was $C_1 - 1$ and the value of C_1 depended on the axial variation of the radius of the cylinder. A uniform axial cylinder took a value $C_1 = \ln 2 - \frac{1}{2} = 0.193$, whereas a prolate spheroid yielded $C_1 = +\frac{1}{2}$. The latter agrees with the results of the exact solution for a spheroid, Equations (7) and (8); in this case the answers are more accurate than the error terms in (9) and (10) indicate.

2.6 Resistive Force Coefficients

The translation of any rigid slender body through a viscous fluid can be fairly readily analyzed by such methods, provided the radius of curvature is large compared with the body radius. In the present context it is useful to view the results by decomposing the velocities of each element relative to the fluid at infinity into normal and tangential components, U_n and U_s , and similarly decomposing the force on that local element into components involving normal and tangential force coefficients as defined in Equations (6). The resulting values of C_n and C_s always take the forms of Equations (9) and (10), but the coefficients C_1 and C_2 are dependent on the overall geometry of the body (through the integration of stokeslets along the entire axis). For example, a circular ring or torus moving in the direction of one of its major diameters takes values of $C_1 = 0.74$, $C_2 = 0.24$ (R. Johnson and T. Y. Wu, private communication).

This is the background for what has come to be known as resistive-force theory in which the force on any element of a slender body such as a cilium or flagellum is calculated from (a) motion of each elemental length of the organelle relative to the fluid at infinity and (b) force coefficients, C_n and C_s , which are determined from the geometry alone.

Hancock (1953) and Gray & Hancock (1955) made a major contribution to research on microorganism movement by applying slender-body theory to the analysis of a flagellum along which travelling waves were propagating (Figure 3). The motion of each individual element relative to the fluid at infinity is thus comprised of a combination of the oscillatory motions due to the passage of the wave and the steady translation of the flagellum through the fluid. The results of Hancock's analyses and the subsequent force coefficients derived by Gray & Hancock (1955) can be interpreted in a simple qualitative way by dividing the axial stokeslet distributions for such a flow into components due to each of these motions and by

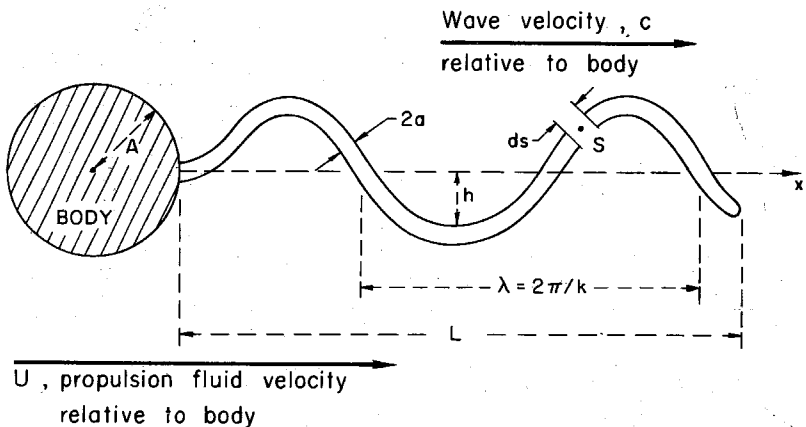


Figure 3 Flagellar propulsion with a planar waveform.

examining primarily the oscillatory motions for these generally involve larger velocities. It follows that the stokeslet distributions due to the oscillatory motions will be harmonic with distance s from the section at which the integrated velocity is being evaluated (see last section). Lighthill has pointed out that this will result in an integral that will converge more rapidly than those that gave terms like $\ln(s_1 s_2/a^2)$ in the last section; indeed, the resulting velocity will instead involve a term like $\ln(\lambda/a)$, so that the wavelength, λ , will be the effective body length rather than the overall flagellar length. The resulting force coefficients according to Gray & Hancock (1955) are

$$C_s = 2\pi\mu \left[\ln\left(\frac{2\lambda}{a}\right) - \frac{1}{2} \right], \quad (11)$$

$$C_n = 2C_s. \quad (12)$$

Recently Lighthill (1975) has shown that the evaluation of the integrals harmonic in s leads to an "effective length" $l^* = 0.09\lambda$, so that

$$C_s = \frac{2\pi\mu}{[\ln(2l^*/a) - \frac{1}{2}]} = \frac{2\pi\mu}{[\ln(2\lambda/a) - 2.90]}, \quad (13)$$

$$C_n = \frac{4\pi\mu}{[\ln(2l^*/a) + \frac{1}{2}]} = \frac{4\pi\mu}{[\ln(2\lambda/a) - 1.90]}. \quad (14)$$

These can, however, be regarded as only approximate; indeed, it is likely that more accurate coefficients, which are presently being sought, will also involve the total flagellar length, L . One indication of this is suggested above, since clearly the stokeslet components due to overall translation of the flagella will contribute terms like $\ln(2L/a)$ as in the case of the translation of rigid slender bodies.

We return later to the consequences of such analyses in the context of the fluid mechanics of biological slender bodies. But the section would not be complete without the addition of one other force coefficient, namely that due to rotation at angular velocity Ω of an element of a slender body about its own axis. Chwang & Wu (1974) have shown that the resulting moment M acting on the body about the axis is simply given by

$$M = C_M \Omega ds; \quad C_M = 4\pi\mu a^2. \quad (15)$$

2.7 Wall Effects on Slender-Body Motions

The resistive coefficients on any body are clearly altered by the presence of a nearby boundary. Moreover, there are many situations in microorganism propulsion and in ciliary mechanics in which the slender bodies operate close to solid boundaries. Examples are (a) effects of the presence of the epithelial wall on ciliary dynamics (Blake & Sleight 1974), (b) the motion of spermatozoa, *in vivo*, either in close proximity to a single wall or within narrow passages, and (c) the effects of a coverslip on studies of microorganism propulsion (Katz 1974 and Winet 1973). Concern about such wall effects has led to a significant number of recent papers on the influence of nearby boundaries on resistive coefficients for slender bodies.

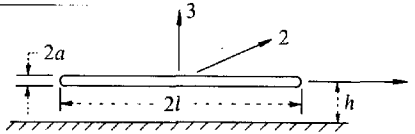
When the distance of the center of the body from the wall, h , is large compared with its length, $2l$, the results of Brenner (1962) for the motion of bodies of arbitrary shape near walls are very useful. Brenner (1962) showed that the wall-affected resistive coefficient (drag/ $2lU$) denoted by C^* was related to the coefficient, C , in the absence of the boundary by

$$\frac{C^*}{C} = \left[1 - Z \frac{C l}{3\pi\mu h} + O\left(\frac{l}{h}\right)^3 \right]^{-1}, \tag{16}$$

where Z was a function only of the geometry and the direction of particle motion. Examples of the numerical values of Z are (a) $Z = 9/16$ for motion parallel to a

Table 2 Wall effects on resistive coefficients for the translation of straight slender cylinders^a

Orientation Parallel to the Wall



$l/h \ll 1$

$l/h \gg 1$

$$C_{s1} = 2\pi\mu \left/ \left[\ln\left(\frac{2l}{a}\right) - 0.807 - \frac{3l}{8h} \right] \right.$$

$$C_{s1} = 2\pi\mu \left/ \left[\ln\left(\frac{2h}{a}\right) \right] \right.$$

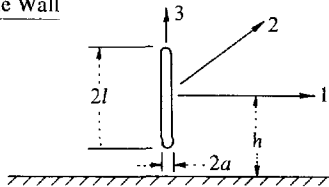
$$C_{n2} = 4\pi\mu \left/ \left[\ln\left(\frac{2l}{a}\right) + 0.193 - \frac{3l}{4h} \right] \right.$$

$$C_{n2} = 4\pi\mu \left/ \left[\ln\left(\frac{2h}{a}\right) \right] \right. \epsilon$$

$$C_{n3} = 4\pi\mu \left/ \left[\ln\left(\frac{2l}{a}\right) + 0.193 - \frac{3l}{2h} \right] \right.$$

$$C_{n3} = 4\pi\mu \left/ \left[\ln\left(\frac{2h}{a}\right) - 1 \right] \right.$$

Orientation Normal to the Wall



$l/h \ll 1$

$l/h \rightarrow 1$

$$C_{n1} = C_{n2} = 4\pi\mu \left/ \left[\ln\left(\frac{2l}{a}\right) + 0.193 - \frac{3l}{4h} \right] \right.$$

$$C_{n1} = C_{n2} \rightarrow 4\pi\mu \left/ \left[\ln\left(\frac{2l}{a}\right) - 0.75 \right] \right.$$

$$C_{s3} = 2\pi\mu \left/ \left[\ln\left(\frac{2l}{a}\right) - 0.807 - \frac{3l}{4h} \right] \right.$$

$$C_{s3} \rightarrow 2\pi\mu \left/ \left[\ln\left(\frac{2l}{a}\right) - 1.75 \right] \right.$$

^aCompiled from Brenner (1962), Katz & Blake (1975), Katz, Blake & Pavari-Fontana (1975), de Mestre (1973), and de Mestre & Russel (1975). Second subscript refers to direction of translation and force.

single solid plane wall, (b) $Z = 9/8$ for motion perpendicular to a single solid plane wall, (c) $Z = 1.004$ for motion parallel to and equidistant between two solid plane walls, and (d) $Z = 2.1044$ for motion along the axis of a cylindrical tube; other useful values are also given by Brenner (1962). First-order, or $O(l/h)$, corrections for wall effects on the resistive coefficients are therefore readily obtained by combination of the result (16) with the coefficients, such as (9) and (10) in the absence of walls. Some examples are listed in Table 2, with Cox's coefficients for slender cylindrical bodies (Cox 1970).

Another general result of particular importance for microorganism propulsion can be readily deduced from Brenner's result; we shall see that the value of the ratio $\gamma = C_s^*/C_n^*$ for a slender element of a cilium or flagellum is of considerable consequence to its propulsive capability. From (16) it is readily seen that the first-order wall effect on this ratio is given by

$$\gamma = C_s^*/C_n^* = \gamma_\infty \left[1 - Z \frac{(C_n^\infty - C_s^\infty) l}{3\pi\mu h} \right], \quad (17)$$

where C_n^∞ , C_s^∞ are resistive coefficients in the absence of the wall or walls and $\gamma_\infty = C_s^\infty/C_n^\infty$. Notice in particular that since $C_n > C_s$ and provided Z is positive, the effect of the nearby boundary always *decreases* γ . Note from Brenner's (1962) quoted values for Z that this quantity is invariably positive for solid boundaries.

When the slender body is closer to the wall so that l/h is no longer small, the geometry of the body becomes important and a more detailed analysis becomes necessary. Katz & Blake (1975) and Katz, Blake & Pavari-Fontana (1975) recently examined this situation by constructing the flow by a distribution of stokeslets along the axis of slender bodies and satisfying the no-slip condition at the wall or walls by adding the appropriate system of image singularities. The resulting integral equations are solved by the techniques developed by Tillett (1970) and Cox (1970). Solutions were obtained for slender cylinders parallel to a single-plane wall and between two plane walls when the distance, h , from the wall is much smaller than the length, $2l$ (but still much greater than the radius a). Their results are included in Table 2; it is significant to note that h now replaces l in the leading term for the coefficient. De Mestre (1973) and de Mestre & Russel (1975) have examined the wall effect for general values of l/h (both large and smaller) and orientations both parallel and perpendicular to the wall. Their results converge asymptotically to the simple results obtained by Brenner's relation at small l/h [provided some typographical errors in de Mestre & Russel (1975) are corrected] and to the results of Katz, Blake & Pavari-Fontana (1975) for parallel slender cylinders. The additional results for perpendicular slender cylinders as $l \rightarrow h$ are also incorporated into Table 2; it is reassuring that if one arbitrarily sets $l/h = 1$ in the expressions for $l/h \ll 1$, then the result differs only slightly from the more exact expressions for $l/h = 1$.

3 PROKARYOTIC CELL PROPULSIVE STRUCTURE AND FUNCTION

The flagella of bacteria are composed of a helical protein, flagellin. From one to eleven strands of flagellin coil together to form a single flagellum sheath (Gerber

1975) which has an amorphous core and a radius of $1.2\text{--}2.0 \times 10^{-6}$ cm. Both motile and fixed-and-stained flagella form a helix that has a pitch range of $1.5\text{--}2.5 \times 10^{-4}$ cm (Lowy & Spencer 1968). Each flagellum is attached to the cell at its base; the attachment site, called the "hook-basal body complex" (DePamphilis & Adler 1971), consists of four rings around the flagellar cylinder, each 2.25×10^{-6} cm in diameter as shown in Figure 4. The most important of these rings are apparently the S and M rings, which are located at the base of the hook.

The contractile mechanism for bacterial flagella has been a subject of recent controversy (Routledge 1975). Doetsch (1966) first proposed the rather startling hypothesis that the material of the flagellum rotates relative to the cell body, indeed that the hook rotates in the cell wall, thus providing a unique example in nature of continuous rotational deformation. Berg & Anderson (1973) and Berg (1974, 1975) have further examined the evidence for, and apparent quantitative features of, this bacterial motor system. The motor seems to consist of rotation of the S and M rings with the flagellum that they carry being driven by some mechanochemical process, presumably akin to the cross-bridge-stepping of heavy meromyosin on actin in striated muscle (Berg & Anderson 1973). However, some recent evidence (Larsen et al 1974) indicates that ATP is not the energy source for this process, so cross-bridge models may be premature. Nevertheless, the basic model of a bacterial flagellar motion appears to be gaining acceptance (Silverman & Simon 1974) at the expense of alternative hypotheses that the contraction consists of a helical wave

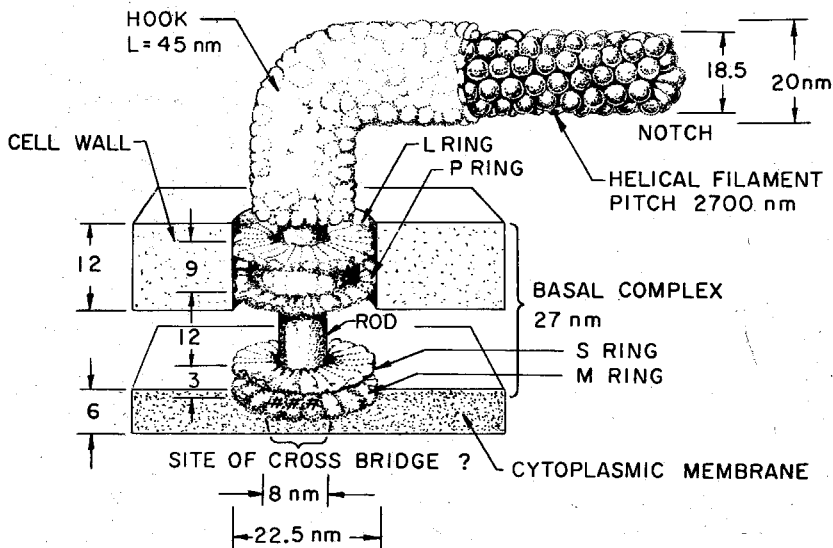


Figure 4 The hook-basal body complex at the junction of a prokaryotic cell and its flagellum. In the rotating-shaft models motion is presumed generated between the M and S portion of the hook and the cytoplasmic membrane. Possible sites of cross-bridges for a model analogous to the muscle sliding mechanism have been indicated. (Adapted from Routledge 1975.)

passing along the flagellum due to propagation of dislocations in the molecular structure of the outer sheath (Harris 1973, Calladine 1974). In terms of the external hydrodynamics of the helical flagellum the two models differ only in the material motion of the surface of the flagellum. In the basal motor hypothesis the flagellum

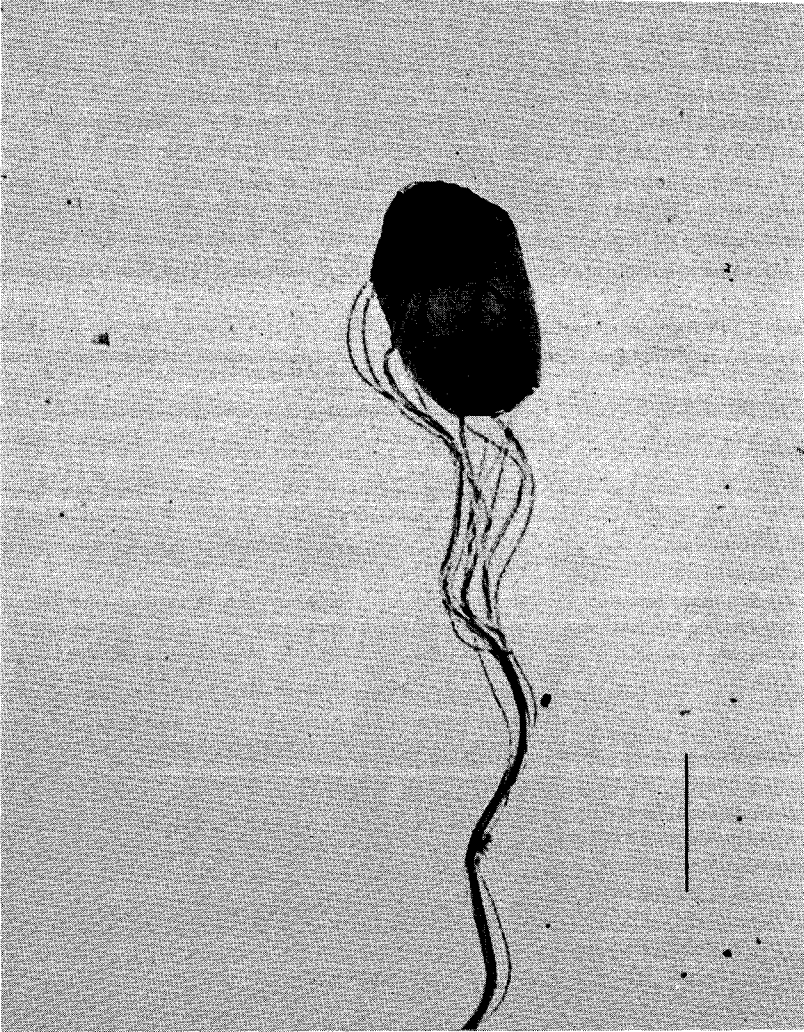


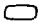
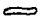
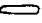












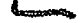


Figure 5 The flagellated bacterium *Salmonella abortus-equi* with its flagella bent aftward and associated in a flagellar bundle (Routledge 1975). This is a fixed specimen. The swimming organism would show less clearance between flagella. The scale bar is $1\ \mu\text{m}$. (We are indebted to Dr. L. M. Routledge for this photograph.)

is basically like a rigid corkscrew rotating relative to the head; in the wave-propagation model the material of the flagellum does not rotate relative to the material of the cell body, but the helix is formed by the helical conformation of the propagated wave. Unless one can observe the material rotation of the flagellum, the two motions appear identical and thus it is difficult to distinguish between them.

Many bacteria (e.g. *Escherichia coli*, *Salmonella*; see Table 3) have several flagella attached at points distributed over the surface of the cell (see Figure 5). When such bacteria are swimming, the separate flagella come together in a synchronous flagellar bundle, which propels the cell (Iino & Mitani 1966). In some strains, periods of concerted swimming are interrupted by brief periods of erratic wobbling ("twiddling"), which may be caused by the fact that the bundle has come apart and each flagellum is acting independently (Macnab & Koshland 1972, Adler 1976). Anderson (1975) has recently discussed the qualitative hydromechanical features of the formation of flagellar bundles.

The close association of rotating flagella in the bundle clearly implies the presence

Table 3 Prokaryote propulsion data

Prokaryote	Body		No. of flagella	Flagellar
	Length (B) (μm) \times width (μm)	Shape		Length, L (μm) or No. of waves \times wavelength
Eubacteria				
<i>Bacillus megaterium</i>	3.0 \times 1.5		~36	2.5 \times 3.9
<i>Bdellovibrio bacteriovorus</i>	1.4 \times 0.25		1	L = 3.4
<i>Clostridium tetani</i>	6.0 \times 0.5		~15	4 \times 1.8
<i>Escherichia coli</i>	3.0 \times 1.5		6	2 \times 2.7
<i>Photobacterium phosphoreum</i>	1.2		1	1.5 \times 3.1
<i>Pseudomonas aeruginosa</i>	1.5 \times 0.5		1	2 \times 1.7
<i>Salmonella typhosa</i>	2.5 \times 0.65		6	4.2 \times 2.5
<i>Sarcina ureae</i>	2.0		1/cell	4 \times 3.2
<i>Serratia marcescens</i>	1.0 \times 0.5		>4	1.5 \times 2.3
<i>Spirillum serpens</i>	3.0 \times 1.0		>14	1.1 \times 2.7
<i>Spirillum volutans</i>	13.5 \times 1.5		>46, 200	1.1 \times 6.5
<i>Thiospirillum jenense</i>	40.0 \times 4.0			—
<i>Vibrio cholera</i>	3.0 \times 0.45		1	1.0 \times 2.4
Spirochaetes				
<i>Cristispira balbianii</i>	80.0 \times 2.0		>100	3.5 \times 6.0
<i>Cristispira</i> sp.	44.0 \times 1.4		—	3.1 \times 14.2
<i>Leptospira icterohemorrhagiae</i>	7.5 \times 0.27		1	—
<i>Spirochaeta litoralis</i>	13.0 \times 0.45		3	1.6 \times 8.2
<i>Spiroplasma citri</i> ^b	6.0 \times 0.16		?	4.1 \times 0.97

^a Flagellum was tethered.

^b Observed in 0.25% agar.

of lubricating layers of fluid between the individual flagella and thus a significant fluid resistance internal to the bundle, especially in the basal motor model; to our knowledge the hydromechanics of this situation has not as yet been closely examined quantitatively, although Berg & Anderson (1973) discount it. Viewed from the exterior fluid the flagellar bundle could be considered as a single slender body whose mean surface rotates relative to the head if the basal motor model is assumed. Thus, whether the principal propulsive unit is a single flagellum or a bundle will have relatively minor effects on the external hydromechanics within the context of a particular contractile process. Finally, it is noteworthy that many bacteria exhibit an increased motility with small increases in viscosity of the surrounding medium and a subsequent decrease with larger increases in viscosity (Schneider & Doetsch 1974 and Shoesmith 1960).

Since the hydromechanics of bacterial flagella is best dealt with in conjunction with the hydromechanics of eukaryotic flagella, we delay the details until Section 4.6.

Table 3 Continued

Bundle		Organism			
Amplitude h (μm)	U/B	U/c	Body rotation, Ω (sec^{-1})	Conditions	References
0.94	6.7	—	600 ^a	19–25°C	139, 183
damped	100	—			173, 208
0.24	—	—			32, 139
0.60	10	—	78 ^a	19–25°C	13, 139, 183
0.40	—	—			32, 139
0.17	40	—	$\Omega/kc = 0.37$	19–25°C	139, 183
0.17	10	—			32, 62, 139
0.38	10	—			139, 183
0.09	30	—			139, 183
0.55	6.7	^b			139, 183
1.47	6.3	^b	20°C	32, 62, 152, 158, 227, 233	
—	0.5	^b	19–25°C	183	
0.17	16.7	—			32, 139, 158
—	—	—			31, 32, 120
1.69	0.36	0.16	300	20°C	31, 55
—	2	—		19–25°C	31, 32, 65, 158, 183
0.84	0.46	0.08	300	20°C	55, 104
0.18	—	—		30°C	67

^aFlagellum was tethered.

^bObserved in 0.25% agar.

4 EUKARYOTIC CELL PROPULSIVE STRUCTURE AND FUNCTION

4.1 Structure of Cilia and Eukaryotic Flagella

Much more is known of the structure and function of cilia and eukaryotic flagella (we use the single word *cilia* for convenience) than is known for prokaryotic flagella. Since there are extensive books and review articles (Gray 1928; Sleight 1962, 1971, 1974a; Holwill 1966a, 1974; Brokaw 1975; Brokaw & Gibbons 1975) on this subject, we attempt only the briefest overview aimed at the fluid mechanician. A typical cross-sectional view of a cilium or eukaryotic flagellum is shown in Figure 6. Within a membrane is the "axoneme," which consists of longitudinal fibrils or tubules (one of the structural elements of which is tubulin) arranged as a number of peripheral pairs plus a central pair. The number of outer pairs is often nine (hence the reference to a "9 + 2" pattern), although many other numbers and modifications of this basic pattern have been observed. "Arms" consisting of dynein project from the outer pairs of fibrils. The dynein and tubulin are believed to interact in a manner analogous to heavy meromyosin and actin in striated muscle, although the precise mechanical details of this interaction have yet to be clearly identified. It has, however, been well established that the energy source, namely ATP, is the same for both systems. The details of the sliding mechanism have not been fully determined as one can gather from the variety of models still being proposed (e.g. Brokaw 1975; Costello 1973a,b; Douglas 1975; Dryl 1975; Harris & Robison 1973; Satir 1974; Summers & Gibbons 1971). An important series of electron microscopy studies by Satir (1965, 1968) and Warner & Satir (1974) have demonstrated that the

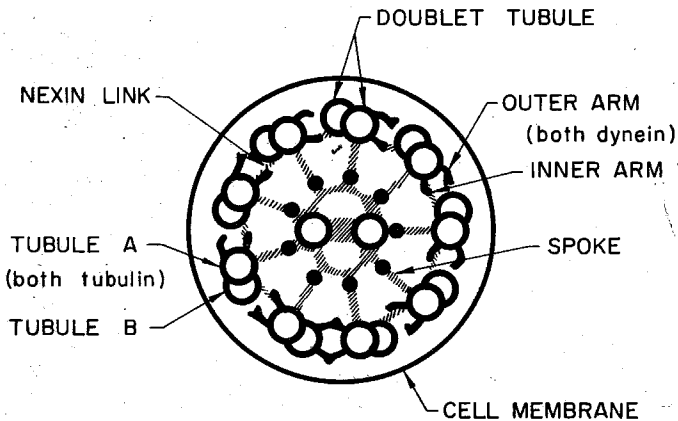


Figure 6 A diagrammatic representation of a cross-section through a cilium (or eukaryotic flagellum). Sliding is generally assumed to be generated longitudinally between the dynein arms and the B tubule across the gap spanned by the nexin link. The active role of the radial spokes in the contraction is not agreed upon. (Modified from Brokaw & Gibbons 1975.)

microtubules remain constant in length during bending and that the bending is associated with longitudinal switching of the "radial spokes"; Figure 7 (from Warner & Satir 1974) is a particularly good electron micrograph showing the rather faint,

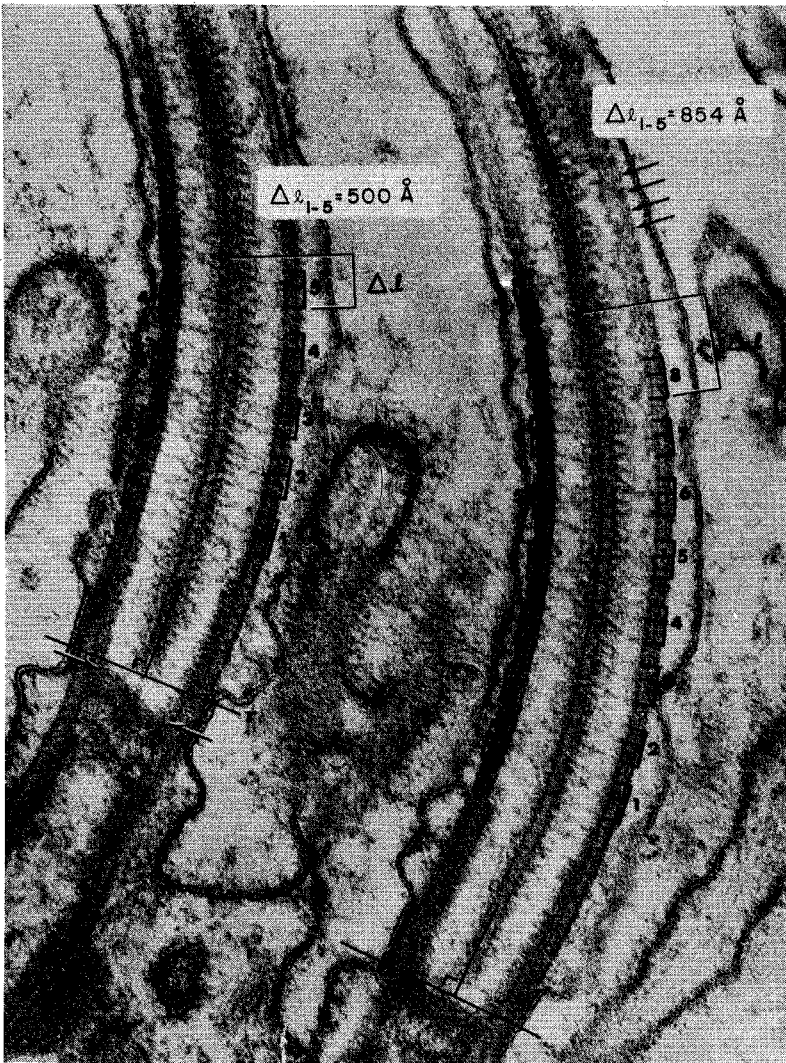


Figure 7 An electron micrograph of two bending cilia, which are longitudinally sectioned and viewed from the side (Warner & Satir 1974). Sliding displacement is indicated by Δl . The right-angle markers denote the upper part of the basal body. The radial spokes are the faint lines extending out from the core of each cilium. The cilia are about $0.18 \mu\text{m}$ wide. (We are indebted to Dr. F. D. Warner for this photograph.)

though visible, spokes on two bent cilia. These investigators have concluded that the radial spokes and their attachment to the central fibers are an important component in the generation of the sliding of peripheral subfibers past one another.



Figure 8 A sea urchin (*Tripneustes gratilla*) spermatozoon extruding microtubules by active sliding following treatment with ATP (Summers & Gibbons 1971). Scale bar is 10 μm . Note the two subfibers coiling as they are extruded. (We are indebted to Dr. K. E. Summers for this photograph.)

In an important series of physiological studies Summers & Gibbons (1971) have demonstrated the sliding phenomenon by inducing spermatozoa whose membranes have been partially digested to extrude subfibers by treating them with ATP; Figure 8 (from Summers & Gibbons 1971) shows this extrusion by sliding dramatically. These investigators propose that the total sliding force is generated between the dynein arms on one pair of peripheral fibrils and subfibril B of the adjacent pair. The discovery of motile spermatozoa lacking central fibrils (van Deurs 1974) appears to support the Summers & Gibbons form of the model. A more extensive account of the development of the "sliding filament" model since its proposal by Machin (1958) may be found in Brokaw & Gibbons' (1975) review.

It is evident that the actively generated bending moment in the contracting cilium is balanced by an internal resistance to motion (both elastic and viscous) and by the external viscous resistance. In this review we concentrate on the evaluation of the latter quantity, although it should be borne in mind that in the mechanics of cilia both elastic and viscous internal forces also appear to play significant roles and must be included in any attempt to extract knowledge of the basic activating force from knowledge of the motions of cilia and the fluid flow they create (see for example Brokaw 1970, 1971, 1972). The base of a cilium or eukaryotic flagellum is firmly imbedded in the cell membrane, and there is no question of relative motion between that base and the cell membrane as there was for prokaryotic flagella; propulsion is always achieved by propagation of waves along the cilia or flagella. The energy source for the motion, namely ATP, may either diffuse along the length of the flagellum or be diffused in from the surrounding fluid. Therefore, the principal unknown is the control mechanism. Much of the recent work has been directed toward identifying the control and feedback systems evidently associated with eukaryotic flagella and cilia (Sleigh 1966, 1969; Brokaw & Gibbons 1975).








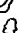





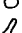
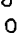








4.2 *Eukaryotic Flagellar Motions*

In this section we concentrate on some of the characteristics of eukaryotic cell propulsion by single organelles, which we continue to call flagella at the risk of confusion with prokaryotic flagella; later we deal with propulsion by multiple organelles such as cilia.

The first fact to emphasize is the great variety of configurations of flagella and organisms (see Jahn & Votta 1972); here we can do no more than indicate some characteristic forms of flagellar motion and identify in particular those with different hydromechanical implications.

Many organisms, including spermatozoa, have long flagella along which they propagate either a planar wave (e.g. *Ceratium*) or a helical wave (e.g. *Trichomonas*) or some combination of the two (see Table 4); typically one finds about two wavelengths along the flagella as illustrated by the multiple exposure of sea urchin sperm in Figure 9 (Brokaw 1965) and the data of Table 4. Commonly the wave is propagated from the base to the tip, although the reverse has also been observed in the trypanosomes (Jahn & Votta 1972). Normally the direction of propulsion is opposite to the direction of wave propagation, although there exist counter examples, especially that of *Ochromonas* (Jahn, Landman & Fonseca 1964). This can

Table 4 Eukaryote propulsion by one to four flagella

Eukaryotes with 1-4 flagella	Body		Flagellum	
	Length (B) (μm) \times width (μm)	Shape	No. of flagella	Length, L (μm) or No. of waves \times wavelength
"Exoflagellates"				
<i>Ceratium fusus</i> ^a	450 \times 22		2	L = 200
<i>Ceratium tripos</i> ^a	225 \times 332		2	2 \times 125
<i>Chilomonas paramecium</i>	35 \times 12		2	1.5 \times ?
<i>Chlamydomonas</i> sp.	13		2	1 \times 6.3
<i>Codonosiga botrytis</i>	15 \times 5		1	L = 30
<i>Dinophysis acuta</i> ^a	65 \times 55		2	L = 65
<i>Dunaliella</i> sp.				
<i>Euglena gracilis</i>	45 \times 15		1	L = 45
<i>Euglena viridis</i>	52 \times 17		1	1.5 \times 35
<i>Gonyaulax polyedra</i> ^a	48 \times 45		2	
<i>Gyrodinium dorsum</i> ^a	34.5 \times 24.5		2	
<i>Gyrodinium dorsum</i>	34.5 \times 24.5		1	
<i>Menoidium cultellus</i>	45 \times 7		1	1.0 \times 10
<i>Monas stigmata</i>	6		2	L = 3, 15
<i>Monas stigmata</i>	6		2	L = 3, 15
<i>Ochromonas malhamensis</i>	3		1	2.8 \times 7
<i>Peranema trichophorum</i>	55 \times 12		2	L = 40
<i>Polytoma uwella</i>	22 \times 11		2	L = 39
<i>Polytoma uwella</i>	22 \times 11		2	
<i>Polytomella agilis</i>	9.8 \times 4.9		4	L = 8.5
<i>Rhabdomonas spiralis</i>	40 \times 10		1	1.0 \times 15
<i>Strigomonas oncopelti</i>	8.2 \times 2.6		1	L = 17
<i>Trypanosoma cruzi</i> ^b	20 \times 2		1	3 \times 3.5
"Endoflagellates"				
<i>Eimeria</i> sp. merozoites	15 \times 1.5		—	1.67 \times 10
<i>Plasmodium berghi</i> sporozoites	10 \times 2		—	L = 8

^a Dinoflagellates with helical flagellum in peripheral groove. Note second *Gyrodinium* has no helical flagellum.

^b Cell body propagates a wave, one wave of 11 μm length.

Table 4 Continued

Flagellum		Organism				
Amplitude <i>h</i> (μm)	Beat form	<i>U/B</i>	<i>U/c</i>	Ω/ω_a	Conditions	References
	helical + planar	0.56			18–20°C	133, 163
	helical + planar	1.11			18–20°C	133, 163
	helical	4.4			26°C, mastigonemes	133, 137, 221
		5.0				116, 143
				$\omega_a = 180$		194, 198
11	helical + planar	sessile			18–20°C, mastigonemes	163, 194
		226/			20.5–21.5°C	83, 116, 133
	helical	3.6				
6	helical	1.5	0.19	0.08		108, 116, 133
	helical + planar	5.2				97, 133
	helical + planar	9.5		$\Omega = 9.4$		99
	planar	4.3		$\Omega = 8.2$		99
3	helical	4.3	0.47	0.06		108
	planar?	45		$\omega_a = 300$	in 3 mm deep chamber	143
	planar?	1.7		$\omega_a = 120$	between thin slides	143
1	planar	19.2		$\omega_a = 430$	18°C, mastigonemes	107
	3-D	0.36			mastigonemes	133, 196
	3-D	3.4			20–22°C	40, 85
	3-D	4.1		$\omega_a = 90$	20–22°C	40, 85
	breast stroke	8.4		0.09	20–22°C	84, 85
3.5	helical	3.0	0.32	0.056	mastigonemes	108, 221
2.4	planar	2.1	0.068	$\omega_a = 110$	22°C	110
0.5	planar	15.2	^b		in blood, flexible body	117
5	planar	0.47			in bile	30
2.9	planar				in salivary gland fluid	219

^aDinoflagellates with helical flagellum in peripheral groove. Note second *Gyrodinium* has no helical flagellum.

^bCell body propagates a wave, one wave of 11 μm length.

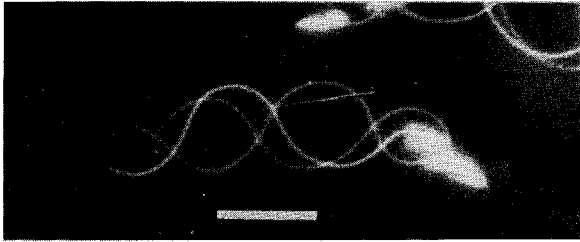


Figure 9 Multiple flash records of swimming tunicate (*Ciona intestinalis*) spermatozoa (Brokaw 1965). The flash rate is 50 Hz and the scale bar is 10 μm . (We are indebted to Dr. C. J. Brokaw for this photograph.)

be explained hydromechanically (Holwill & Sleight 1967, Brennen 1976) because the flagellum of *Ochromonas* has attached to it a large number of rigid projections known as mastigonemes, which move through the fluid in response to the passage of the flagellar wave as indicated in Figure 10 (see Section 4.4).

We have listed some of the observed characteristics of the propulsion systems of eukaryotes with flagella in Tables 4 and 5 and depicted the general features of some spermatozoa in Figure 11 (for planar wave propagation $\omega_a = kc$ in these tables). Note again that few organisms are completely documented and even more rarely are all data for the same organism gathered under similar conditions.

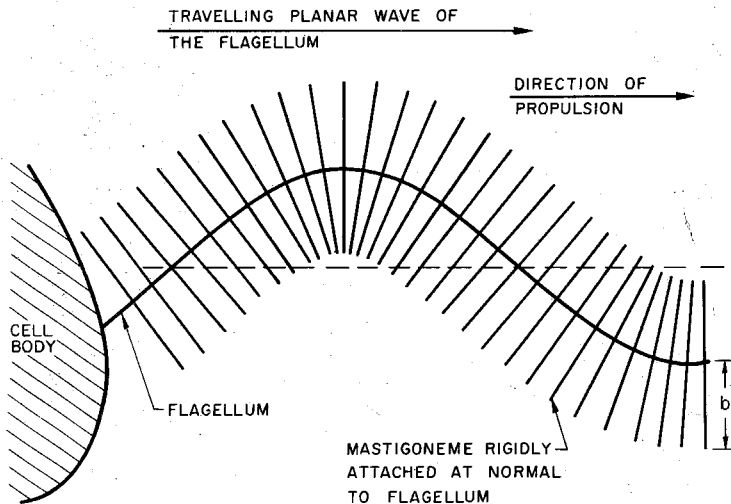


Figure 10 The flagellar/mastigoneme propulsion system.

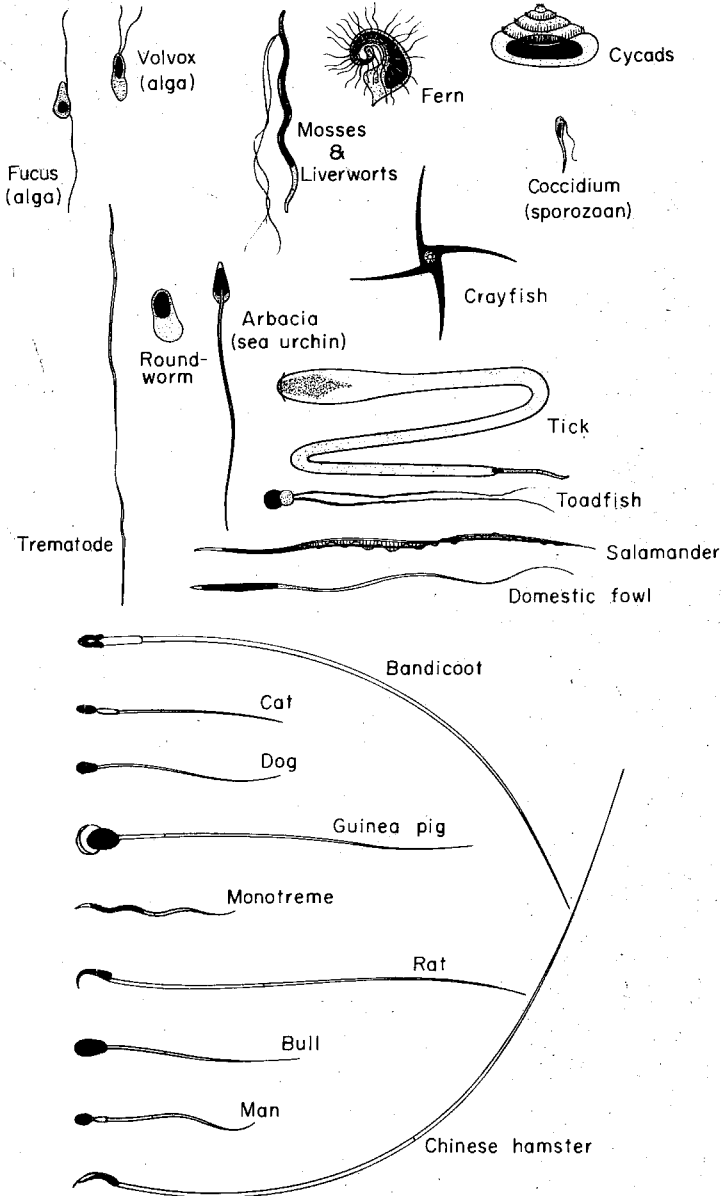


Figure 11. A sampling of the variety of spermatozoon body geometries. The mammalian spermatozoa—from bandicoot downward—are drawn at their relative sizes with the human spermatozoon $40\ \mu\text{m}$ long. (Selected from Austin 1965.)














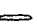
4.3 Hydromechanics of Flagella with Planar Waves

From a point of view of hydromechanical understanding it is simplest to begin by considering the propulsion of an organism by means of a single flagellum propagating planar waves from base to tip. A simple but idealized example might best serve as a starting point for the discussion. Suppose the spherical body of radius, A , of the idealized organism in Figure 3 is propelled by means of a flagellum with planar waves of wavelength λ ($k = 2\pi/\lambda$), and wave amplitude, h , travelling at wave velocity, c relative to the body. We view an element of the flagellum, S , in a frame fixed in the body and assume the motion of S is purely normal to the direction x so that the motion of the element relative to the fluid at infinity (which has a velocity, U , corresponding to the velocity of propulsion) has components normal and tangential to the axis of the slender-body element S given by

$$q_n = U \sin \varphi - khc \cos \theta \cos \varphi, \quad (18)$$

$$q_s = U \cos \varphi + khc \cos \theta \sin \varphi, \quad (19)$$

Table 5 Spermatozoa propulsion

Spermatozoa of	Body		Flagellum
	Length (B) (μm) \times width (μm)	Shape	Length, L (μm) or No. of waves \times wavelength
<i>Bos</i> (bull)	10×5		1×60
<i>Chaetopterus</i> (annelid)	3.4×1.7		1.25×25.4
<i>Ciona</i> (tunicate)	4.1×2.4		1.25×32
<i>Colobocentrotus</i> (sea urchin)	8.2×2.9		1.5×30
<i>Culex</i> (mosquito)	17.1×1.4		3.3×15.7
<i>Didelphis</i> (opposum)			
<i>Mesocricetus</i> (hamster)	13.8×3		$L = 236$
<i>Homo</i> (human)	5.8×3.1		$L = 36$
<i>Lygaeus</i> (milkweed bug)	4.8×1.0		2.3×13.0
<i>Lytechinus</i> (sea urchin)	5.1×2.9		1.25×30
<i>Mus</i> (mouse)	33×5.5^a		1.2×65
<i>Ostrea</i> (oyster)	2.6×2.8		$L = 47$
<i>Ovis</i> (ram)	10.6×6.2		$L = 59$
<i>Psammechinus</i> (sea urchin)	1.0		1.25×24
<i>Tenebrio</i> [mealworm (beetle)]	6.2×1.7		4×11.7

^a Midpiece included in "body."

where $\theta = k(x - ct)$ and $\tan \varphi = kh \cos \theta$. If we then assume known resistive coefficients C_n and C_s , the force on the element of length ds in the x direction is

$$C_n ds [U - (1 - \gamma)U \cos^2 \varphi - (1 - \gamma)khc \cos \theta \cos \varphi \sin \varphi] \tag{20}$$

at each instant in time where $\gamma = C_s/C_n$ is the ratio of the resistive coefficients. From an integration over one cycle in time it follows that each element is subject to a mean force in the positive x direction which can be integrated over the length L of the flagellum to yield a mean force on the flagellum equal to

$$C_n L [U - (1 - \gamma)c - (1 - \gamma)(U - c)(1 + k^2 h^2)^{-1/2}]. \tag{21}$$

If the organism were self-propelling, this would be equal to the drag $6\pi\mu UA$ on the head. Hence the propulsive velocity U is

$$\frac{U}{c} = \frac{(1 - \gamma)(1 - \beta)}{(1 - \beta + \gamma\beta + \delta)} \tag{22}$$

where $\beta = (1 + k^2 h^2)^{-1/2}$ and $\delta = 6\pi\mu A/LC_n$. On the other hand, if the organism

Table 5 *Continued*

Flagellum		Organism				
Amplitude h (μm)	Beat form	U/B	U/c	Ω/ω_a	Conditions	References
11	3-D	9.7	0.075	$\omega_a = 135$	37°C, $\mu = 1$ cp	46, 170, 186
3.8	2-D	30.8	0.156	$\omega_a = 166$	16°C, $\mu = 1.4$ cp	41, 46
4.3	3-D & 2-D	40.2	0.147	$\omega_a = 220$	16°C, $\mu = 1.4$ cp	41, 46
2.8	2-D	27.8	0.237	$\omega_a = 200$	25°C, ATP reactivated	46, 81
6.4		0.36				165
	3-D				37°C, swim as pairs	164
	3-D			0.2	37°C	164
	3-D	8.6		0.5	37°C, U decreases 46% in cervical mucus	103, 164
2.1						165
4.6	2-D	31.0	0.185	$\omega_a = 180$	16°C, $\mu = 1.4$ cp	41, 46
15	3-D			0.5	37°C	164
4.7	2-D ^b	63.0		$\omega_a = 270$	23°C	70
	3-D					
7.4	2-D ^b	12.8		$\omega_a = 180$	35.5°C	70
	3-D					
4	2-D	190		$\omega_a = 220$		91, 93
4.2	2-D?	16.1	0.33	$\omega_a = 176$		6, 165

^b Waves formed by flagellar beat are two-dimensional near a boundary (slide glass) and three-dimensional far from the boundary.

were restrained from moving, the thrust, T , developed by the flagellum in the positive x direction follows directly from (21) with $U = 0$ and is

$$\frac{T}{6\pi\mu Ac} = \frac{(1-\gamma)(1-\beta)}{\delta} \quad (23)$$

Lighthill (1975, p. 55) shows that the results for more general waveforms do not differ from the above, provided one uses a more general definition for β as the mean value of the square of the tangential direction cosine of the waveform.

These results show the primary dependence of the performance of the flagellum on the wave velocity, c , the resistive-force-coefficient ratio $\gamma = C_s/C_n$, and the nondimensional wave amplitude, kh . The performance is clearly enhanced by decrease in both γ and β (the latter arising from increasing kh) not only in terms of uniform translational motion as given by U/c but also from the point of view of acceleration from rest and maneuverability, both of which could be characterized by T . Although there has been a tendency for the fluid-mechanical analyses to concentrate on the optimization of the propulsive system in terms of seeking that which would give maximum rectilinear propulsion per unit energy expenditure, it is not at all clear that this is necessarily the most important feature of the system for any particular microorganism. Indeed the ability to accelerate and maneuver could be an asset as important, if not more important, to the organism.

According to the relations (22) and (23), U/c and $T/6\pi\mu Ac$ increase monotonically with decreasing β or increasing nondimensional wave amplitude kh approaching asymptotic values of $(1-\gamma)/(1+\delta)$ and $(1-\gamma)/\delta$, respectively, for large kh . But the penalty paid for these enhanced propulsive effects is an increase in the energy required; the mechanical rate of work being done on the fluid can readily be obtained by integrating the increment of rate of work done per unit flagellar length $C_n(q_n)^2 + C_s(q_s)^2$ over one cycle of time and summing for the entire length of the flagellum. Lighthill (1975) has shown that this leads to a maximum efficiency of rectilinear propulsion by a general planar wave when

$$\beta = \gamma^{1/2}(1+\delta)/[\gamma + \delta + \gamma^{1/2}(1+\delta)], \quad (24)$$

for which $U/c = (1-\gamma^{1/2})/(1+\delta)$. Furthermore, this optimum value of β is rather insensitive to the values of either γ or δ and takes values for $\gamma = \frac{1}{2}$ of 0.586 for very small δ (i.e. an organism with a small cell body, A) and 0.471 for very large δ (i.e. an organism with a large cell body). In the case of a sinusoidal waveform, these values correspond to nondimensional wave amplitudes kh of 1.37 and 1.88, respectively, and it is of interest to observe that many organisms with planar flagellar waves appear to operate with wave amplitudes of this order. Similarly it is instructive to examine the maximum mean propulsive force in one direction that can be generated by a small element of a slender body whose position can oscillate sinusoidally in time within one plane and whose angle of inclination in that plane is also allowed to oscillate sinusoidally. One finds that the optimum propulsive force per unit energy expenditure occurs when the position oscillates normal to the direction of the required thrust, the mean inclination to this direction is zero, and the inclination oscillation is $\pi/2$ out of phase with the position oscillation. This corresponds precisely to the form of motion in a travelling wave, and one further

finds that the optimum amplitude of the inclination oscillation, θ , is 63.9° , which for a sinusoidal travelling wave yields a value for kh of 2.

Gray & Hancock (1955) examined the propulsion for sea urchin spermatozoa (*P. milians*), which propagates a particularly sinusoidal waveform (see Figure 9), and observed an average propulsive velocity of $191.4 \mu\text{m sec}^{-1}$, in excellent agreement with a value of $191 \mu\text{m sec}^{-1}$ computed by using the observed wave amplitude, length, and velocity and an expression similar to Equation (22) with $\gamma = 0.5$. Lighthill has since suggested, and Gray & Hancock were probably aware, that such agreement was in some sense fortuitous and misleading. First, the more sophisticated analysis of Hancock (1953) [see also Lighthill (1975) and Section 2.5] suggests that a more accurate value of γ is significantly higher (about 0.7), which in view of the factor $(1-\gamma)$ in the expression (22) would cause significant disagreement. On the other hand, Gray & Hancock (1955) do mention that propulsion was occurring in close proximity to either the glass or the air surface; from Section 2.6 we have seen that the value of γ could be significantly reduced and propulsion enhanced by the proximity of a boundary and it would seem that the net result is a γ of order 0.5.

The last observation serves further to illustrate the difficulty of wall effects upon data obtained in the confined fluid of a microscope slide; it also further exemplifies the beneficial propulsive effect that can be obtained by a flagellated organism moving close to a solid boundary. The recent detailed analyses of this problem by Katz (1974) yielded further information on these wall effects for flagellated organisms. The results do not differ qualitatively from those expected on the basis of the result (17), although Katz has examined the waveforms on the flagellum that would lead to the maximum benefit in the presence of a boundary.

In concluding this section we must remark that while the simplicity of the resistive-force theory is a boon to biologists seeking approximate estimates, many potentially significant hydromechanical effects have been neglected in such an approach. First, there is the previously discussed uncertainty in the force coefficients, C_n and C_s , which in reality implies the necessity of abandoning such a simplistic approach in order to seek more accurate solutions. Secondly, the effect of the often large cell body on the flow experienced by the flagellum has been entirely neglected and is a problem clearly in need of attention. A more accurate analysis will require construction of the entire flow field due to both the cell body and the beating flagellum by means of fundamental singularities. Further evidence for the necessity of such an approach is provided by the observations of the flow field near a flagellum obtained by Lunec (1975). Lunec compared the actual flow near the flagellum of *Crithidia oncopleti* (as visualized by tracer particles) with a theoretical reconstruction based on a distribution of stokeslets along the flagellar axis, whose strength was obtained from Gray & Hancock's resistive-force coefficients. The resulting fluid velocities were in marked disagreement, and Lunec concluded that this could in part be due to the proximity of the cell body.

4.4 *Hispid Flagella*

Some eukaryotic organisms such as *Ochromonas* (Figure 10), which propagate planar waves, have rigid projections known as mastigonemes, which protrude from the flagellum. These mastigonemes move through the fluid as the waves pass along the

flagellum, and their net effect is to propel the organism in the direction opposite to that which would occur in the absence of mastigonemes. Jahn, Landman & Fonseca (1964) suggested that a simple way of viewing the hydromechanical effect of the mastigonemes is that they increase C_s much more than C_n , resulting in values of γ greater than unity and thus propelling the organism in the direction opposite to that which occurs when $\gamma < 1$ [Equation (22)]. It is, however, a simple matter to apply resistive theory to the mastigonemes as Holwill & Sleight (1967) and Brennen (1976) have done and to show that for rigid mastigonemes the result (22) is altered to

$$U/c = -(1-\beta)(\delta-\alpha)/(\delta+2\alpha+2\delta\alpha+\beta\delta-\beta\alpha), \quad (25)$$

where $\alpha = 6\pi\mu A/C_n^m bn$, and n , b , and C_n^m are respectively the number, length, and normal resistive coefficient of the mastigonemes. Here γ has been assumed to be one half for both flagellum and mastigonemes. Clearly if the total length of all the mastigonemes together (bn) is greater than the flagellum length so that $\delta > \alpha$, then U/c is always negative and an organism with a hispid flagellum moves with its flagellum forward while propagating waves along the flagellum in the same direction. The result (25) yields a value of $60 \mu\text{m sec}^{-1}$ for *Ochromonas*, which is in good agreement with the observed values of $55\text{--}60 \mu\text{m sec}^{-1}$ (Holwill & Sleight 1967); Brennen (1976) has also examined the case of flexible mastigonemes and concluded that while the mastigonemes of *Ochromonas* are probably thick enough to have sufficient rigidity for hydromechanical purposes, the smaller "hairs" on *Euglena* flagella are probably so flexible that they have little hydromechanical effect.

4.5. Helical Flagellar Propulsion

The propagation of a helical wave along any flagellum, as illustrated in Figure 12, gives rise to a net torque on the flagellum about the longitudinal axis; this causes the cell body to rotate (the *material* of the flagellum must rotate with the same angular velocity) so that an equal and opposite torque on the cell body is generated and the total torque on the organism is zero as it must be from mechanical first

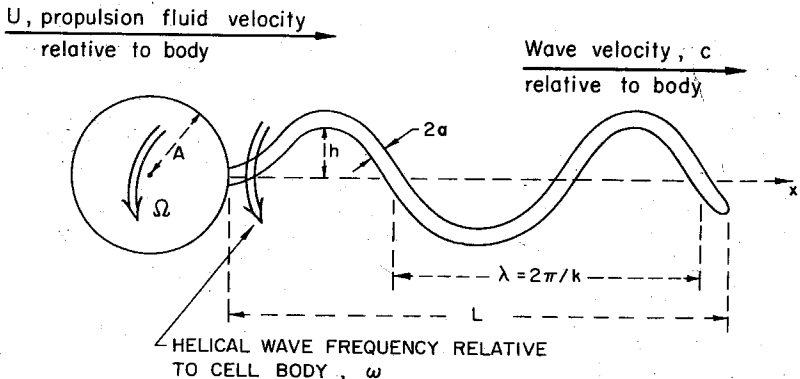


Figure 12 Flagellar propulsion with helical waveform.

principles. Although this point was fully appreciated by Gray (1953), it was left unresolved in some of the early resistive-theory analyses by Holwill & Burge (1963) and Holwill (1966b). Chwang & Wu (1971) (see also Schreiner 1971) first presented a complete solution in which both the condition of zero total longitudinal force and the condition of zero total torque were applied to obtain not only the ratio of the forward speed, U , to the helical wave velocity, c (relative to the cell body), but also the ratio of the angular velocity of spin of the cell body (equal to the material rotation of the flagellum), r , to the angular velocity of the helical wave propagation relative to cell body, ω (equal to kc where $k = 2\pi/\lambda$ and λ is the wavelength of the helical wave). These interconnected results are

$$\frac{c}{U} = \frac{1 + 2k^2h^2 + A^*}{k^2h^2} \left\{ 1 + \frac{2(1 + k^2h^2)^2 + (2 + k^2h^2)A^*}{(1 + 2k^2h^2 + A^*)B^*} \right\}, \quad (26)$$

$$-\frac{\omega}{\Omega} = 1 + \frac{(1 + 2k^2h^2 + A^*)B^*}{2(1 + k^2h^2)^2 + (2 + k^2h^2)A^*}, \quad (27)$$

where we have changed the sign of the second expression by defining values of ω and Ω to be positive in the same rotational sense in order to highlight the fact that, as a result of the torque balance, ω and Ω are naturally of opposite sign. In the above expressions h is the helical wave amplitude and

$$A^* = 3\mu A(1 + k^2h^2)^{1/2}/2\pi LC_s,$$

$$B^* = 4\mu[\pi a^2 + A^3(1 + k^2h^2)^{1/2}/2\pi L]/h^2C_s,$$

where A is the radius of the cell body (assumed spherical), L is the distance from the cell body to the end of the flagellum, a is the radius of the circular cross-section of the flagellum, and C_s is the tangential resistive coefficient. It was assumed that $\gamma = C_s/C_n$ was equal to 1/2. These results show interesting asymptotic limits; with a vanishingly small head ($A \rightarrow 0$) the forward propulsion given by U/c will become small and the material tends to rotate with a velocity, Ω , almost equal and opposite to the angular wave velocity, ω . This particular limit has relevance to the propulsion of a spirochete, which, lacking a flagellum, propels itself by propagating a helical wave along its long thin body; apparently the torque arising from the helical wave is balanced by an opposite rotation of the surface of the body (Chwang, Winet & Wu 1974; Kaiser & Doetsch 1975; Wang & Jahn 1972). On the other hand, for a large cell body Ω tends to zero, but the propulsive velocity again becomes small due to the large drag on the cell body. Between these limits a maximum value of U/c occurs. For typical values of kh and kb of 1 and 0.1, respectively, this maximum occurs when the "head-to-tail" ratio, A/a , is between 10 and 20, which is apparently typical for many organisms.

As far as the helical flagellar propulsion of eukaryotic cells is concerned, there have been few comprehensive comparisons of the theory with observations; the obvious difficulty is that the material rotation, Ω , is extremely difficult to observe or measure. Some partial analysis for *Euglena* by Holwill (1966b) did, however, appear to yield propulsive velocities of the same order of magnitude as those

observed, and the results of Chwang, Wu & Winet (1972) and Winet & Keller (1976) provide a detailed analysis of a more complex form of propulsion, namely that associated with the prokaryote *Spirillum*. In Tables 4 and 5 we have compiled some of the known data on eukaryote propulsion by flagella; invariably the helical wave propagation frequency quoted is the apparent wave frequency, ω_a , seen by the observer, and it should be noted that according to the present definitions for helical waves $\omega_a = \Omega + \omega$.

4.6 Prokaryotic Flagellar Propulsion

The above analysis applies to helical eukaryotic flagella and requires modification as far as prokaryotic flagellar propulsion is concerned; wave propagation along the flagellum should be replaced by relative material rotation between the cell body and the flagellum if the basal motor model is to be accepted. Although the results for this case do not appear explicitly in the literature, they should be readily obtained by the same methods used by Chwang & Wu (1971), and one can anticipate that the results will only differ from (26) and (27) because of the torque created by the different angular velocities of the material of the flagellum. The effect is probably small when the cell body is relatively large, and the torque due to the motion of the flagellar element through the fluid in an azimuthal direction is much larger than the torque due to flagellar material rotation.

Shimada, Yoshida & Asakura (1975) made a complete set of measurements for the bacteria *Salmonella* (many flagella forming a bundle) and *Pseudomonas* (single flagellum) and compared their observations with the expressions (26) and (27). The proper comparison might be with the expressions modified as suggested above; nevertheless, it is of interest to observe that while the agreement in the case of *Pseudomonas* appeared reasonable, the theory gave significantly lower values for U/c than those observed for the multiflagellated *Salmonella*. Although other explanations are possible, these results suggest that the effective γ for a flagellar bundle may be significantly less than $1/2$, a not unreasonable possibility.

5 THE HYDROMECHANICS OF CILIARY SYSTEMS

5.1 Ciliary Motions

In the previous section we discussed the hydromechanics of locomotion in organisms propelled by individual flagella or flagellar bundles. In some organisms with more than one flagellum the hydromechanical analysis could proceed along similar lines, provided the hydrodynamic interactions between the flagella are relatively weak. However, there are organisms with more than one flagellum that seemingly derive a beneficial propulsive effect by adjustment of the phase relationships of the beat patterns of their "flagella" [for example *Mixotricha* (Cleveland & Cleveland 1966) and *Volvox* (Hand & Haupt 1971)]. It appears that such beneficial interactions can also accrue to groups of individual organisms swimming close to one another; there are clearly analogous natural phenomena at high Reynolds numbers in the flight patterns of groups of birds and in the schooling of fish (Weihs 1975).

Cilia are essentially short flagella, which may beat back (recovery stroke) and forth (effective stroke) at different rates transcribing what is known as a "polarized"

beat or which may oscillate in a manner indistinguishable from "eukaryotic flagella." They occur in large arrays, such as "ciliated epithelium," and produce fluid motion by collaborative action arising from a definite phase relationship between the beats of neighboring cilia. The presence of such a relationship is known as metachrony, which often results in a wave, known as a metachronal wave, travelling over the array. It may be that ciliary systems evolved from flagella, because of the beneficial hydrodynamic effects of the interactions of the cilia.

Cilia occur throughout the animal kingdom and indeed are extensively used not only for producing fluid motion but also for sensing motion. Examples of the former use are the cilia in the gills of nonmotile marine animals, used for ingestion of water (Aiello & Sleight 1972, Sleight & Aiello 1972), and the cilia lining the trachea and lungs that provide a cleaning mechanism by continuously propelling mucus up and out of the lungs. (Figure 13 is an electron micrograph of the cilia of frog lung mucosa.) Cilia also line the oviduct and contribute to the transport of the ova in that organ (Halbert, Tam & Blandau 1976; see also Dirksen & Satir 1972); the uterine wall is ciliated and the fact that spermatozoa appear to swim close to this wall may be because they derive a beneficial effect from the beating cilia. In addition, the cilia on the membrane lining the ventricles of the brain (the ependyma) have

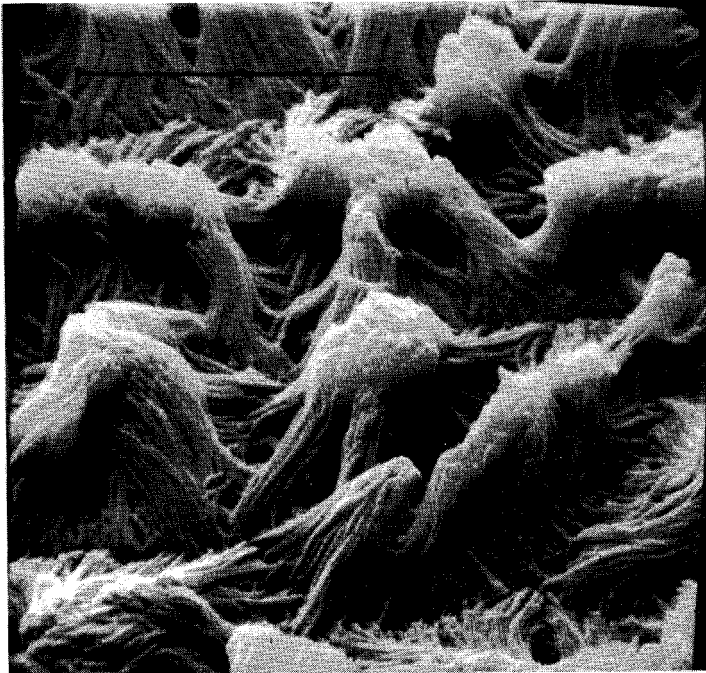


Figure 13 A scanning electron micrograph of frog respiratory mucosa. These fixed organelles display a typical metachronal pattern that reflects the beat-rhythm orientation. Scale bar is 10 μ m. (We are indebted to Dr. P. P. C. Graziadei for this photograph.)

beat or which may oscillate in a manner indistinguishable from "eukaryotic flagella." They occur in large arrays, such as "ciliated epithelium," and produce fluid motion by collaborative action arising from a definite phase relationship between the beats of neighboring cilia. The presence of such a relationship is known as metachrony, which often results in a wave, known as a metachronal wave, travelling over the array. It may be that ciliary systems evolved from flagella, because of the beneficial hydrodynamic effects of the interactions of the cilia.

Cilia occur throughout the animal kingdom and indeed are extensively used not only for producing fluid motion but also for sensing motion. Examples of the former use are the cilia in the gills of nonmotile marine animals, used for ingestion of water (Aiello & Sleigh 1972, Sleigh & Aiello 1972), and the cilia lining the trachea and lungs that provide a cleaning mechanism by continuously propelling mucus up and out of the lungs. (Figure 13 is an electron micrograph of the cilia of frog lung mucosa.) Cilia also line the oviduct and contribute to the transport of the ova in that organ (Halbert, Tam & Blandau 1976; see also Dirksen & Satir 1972); the uterine wall is ciliated and the fact that spermatozoa appear to swim close to this wall may be because they derive a beneficial effect from the beating cilia. In addition, the cilia on the membrane lining the ventricles of the brain (the ependyma) have

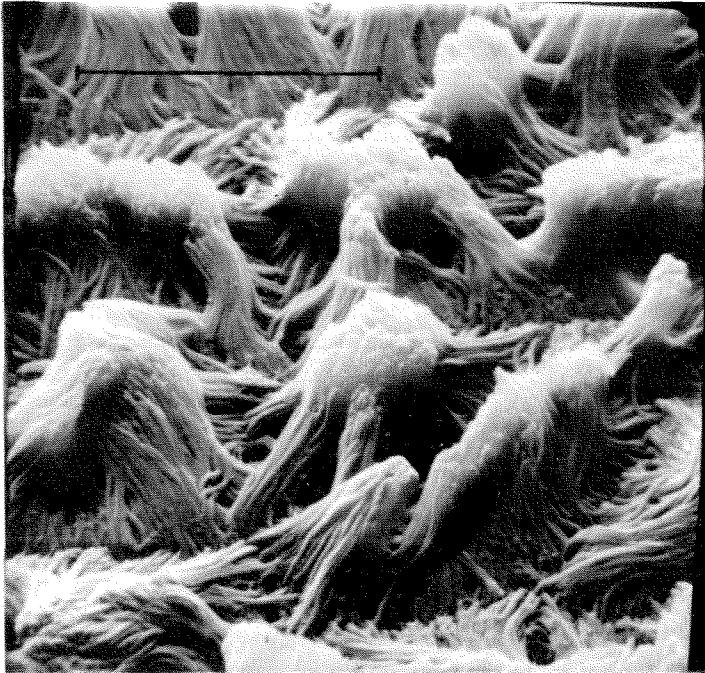


Figure 13 A scanning electron micrograph of frog respiratory mucosa. These fixed organelles display a typical metachronal pattern that reflects the beat-rhythm orientation. Scale bar is 10 μm . (We are indebted to Dr. P. P. C. Graziadei for this photograph.)

been shown to create sufficient local mixing to affect the thickness of the so-called unstirred layer, thereby enhancing the diffusion or transport of ions across the membrane (Nelson 1975). There has been little detailed hydrodynamic analysis of this system. Other functions in which motile cilia play a major role are cited in Table 1. So-called sensory cilia tend to be nonmotile and often display a 9+0 microtubular axoneme. They are found in sensory organs devoted to photoreception ("eyes"; the flagellum of some protozoa is also part of a photoreceptor system: e.g. Hand & Haupt 1971), chemoreception (olfactory organs: e.g. Reese 1965), and mechanoreceptors, which are adapted for detection of sound, touch, or orientation in a gravity field. In no case has it been demonstrated that the cilia are in fact "transducers" of stimulus energy into nerve transmission energy (Barber 1974). They all appear to "sensitize" the cells carrying them for the transduction process by either (a) distortion of the membrane so as to produce changes in the molecular organization of the excitable area, which cause changes in ion permeability leading to a depolarization, (b) deformation of adsorbed mucus so as to give rise to piezoelectric potential differences, or (c) initiation of electrical changes, which result from some "inherent mechanosensitivity" in the cilia (Barber 1974). Understanding of the operation of sensory cilia is beyond the limits of a strictly fluid-mechanical analysis, but the fluid mechanician needs to be aware of these limits to keep his analysis in perspective. The importance of ciliary systems extends even into ecological areas. For example, an individual California mussel *Mytilus californianus* can remove a significant amount of suspended mud and other matter from water, given an average filtration rate of 2.6 liters of water per hour through its cilia-lined gills (Fox & Coe 1943).

But perhaps the ciliary systems most readily observed are those that provide propulsion for eukaryotic cells (e.g. Figures 14 and 15). A sampling of the propulsive parameters of such cells is presented in Table 6. From a hydrodynamic point of view these systems are more readily understood because the fluid is usually Newtonian, or at least is readily adjusted to be Newtonian without placing the organism in an unusual environment. On the other hand, the fluid in mammalian ciliary systems is often highly non-Newtonian (e.g. the mucus in the lung). Although we concentrate here primarily on the locomotion of ciliated organisms, the future extension of the knowledge gained to the understanding of other ciliary systems in nature should be borne in mind.

Each individual cilium usually has a fairly regular beat pattern (see, for example, Sleight 1960, 1962, 1968, 1972, 1973, 1974c; Parducz 1967), which often appears to be created by the propagation of a bend from the base to the tip of the cilia as illustrated by the beat pattern for *Opalina* in Figure 16. That phase of the beat in which each cilium is moving in a general direction so as to propel the organism is termed the *effective stroke*. Generally the cilium is straightened out during this phase and in the remainder of the beat known as the *recovery stroke* the cilium sneaks back to its starting point in a bent position so that a significant portion of each cilium is moving tangential to the fluid rather than normal to it as in the effective stroke. Such asymmetry immediately suggests that the cilia are taking advantage of the difference in the force coefficients for flow normal and tangential

to a slender body. Furthermore, the motion is often three-dimensional with some recovery motion taking place out of the plane of the effective stroke, as is the case with *Paramecium* (Machemer 1972a,b; Tamm 1972). While precise information on the ciliary beat pattern represents necessary data prior to any hydrodynamic analysis, it is difficult to obtain from light microscopy studies. In this respect the beautiful electron microscopy studies originated by Tamm & Horridge (1970) and Tamm (1972) greatly add to our knowledge of ciliary motion (see Figures 14 and 15).

Often eukaryotic cilia ensembles exhibit metachrony: in one surface direction a cilium beats slightly out of phase with its neighbor so as to produce a metachronal wave (velocity, c) travelling over the surface (see Figure 14). To add to the complexity the direction of wave propagation may have almost any orientation relative to the direction of the effective stroke. Knight-Jones (1954) coined a series of terms to identify this relationship: when the metachronal wave propagation and the effective stroke are in the same direction, this is known as *symplectic* metachronism; if they are in opposite directions, it is termed *antiplectic*; and if the directions are normal to one another they are termed *diaplectic* (*dexioplectic* if the rotation from the metachronal wave direction to the effective stroke direction is 90° anticlockwise viewed from above and *laeoplectic* if 90° clockwise). Symplectic metachronism is illustrated by the electron micrograph of Figure 14 (Tamm & Horridge 1970) and the upper part of Figure 16 for *Opalina*; the lower part of Figure 16 represents an antiplectic approximation to the beat pattern of *Paramecium*, which does, however, contain a dexioplectic component as indicated in the electron micrograph of Figure 15 (Tamm 1972). On the other hand, there are ciliary systems in which metachrony is indiscernible. For example, Cheung & Jahn (1975) could not detect any organized metachrony in rabbit tracheal cilia, and Figure 17 from the frog's olfactory epithelium shows almost random cilia orientation (Graziadei 1971); on the other hand, another scanning electron micrograph from Graziadei (1971) of the cilia in the lung mucosa of the frog shows clear metachronism (Figure 13).

Many organisms have an avoidance response in which they reverse the direction of metachronal wave propagation and thus their direction of motion, a phenomenon known as ciliary reversal (Jahn 1975). This appears to be linked to their longitudinal electropotential gradient since it can be achieved by external imposition of an electrical potential. Other organisms such as *Opalina* appear able to vary continuously the direction of wave propagation and thus achieve greater maneuverability (Sleigh 1962). These responses in organisms with no identifiable and separate nervous system merely serve to highlight one of the great puzzles of ciliary systems, namely how these delicate phase relationships between the cilia are controlled. If one had to build a mechanical model to simulate such a system it would be extremely difficult, which probably accounts for the singular lack of mechanical model studies [the early work of Miller (1966) is the only work of this kind that we know of]. Nervous control of ciliated epithelium is one of the important problems to which these studies may be applied. In this context it may be noted that Murakami & Takahashi (1975) have shown that transient depolarization of the cell carrying the cilia by nervous activity is correlated with the "quick-arrest response" of the cilia.

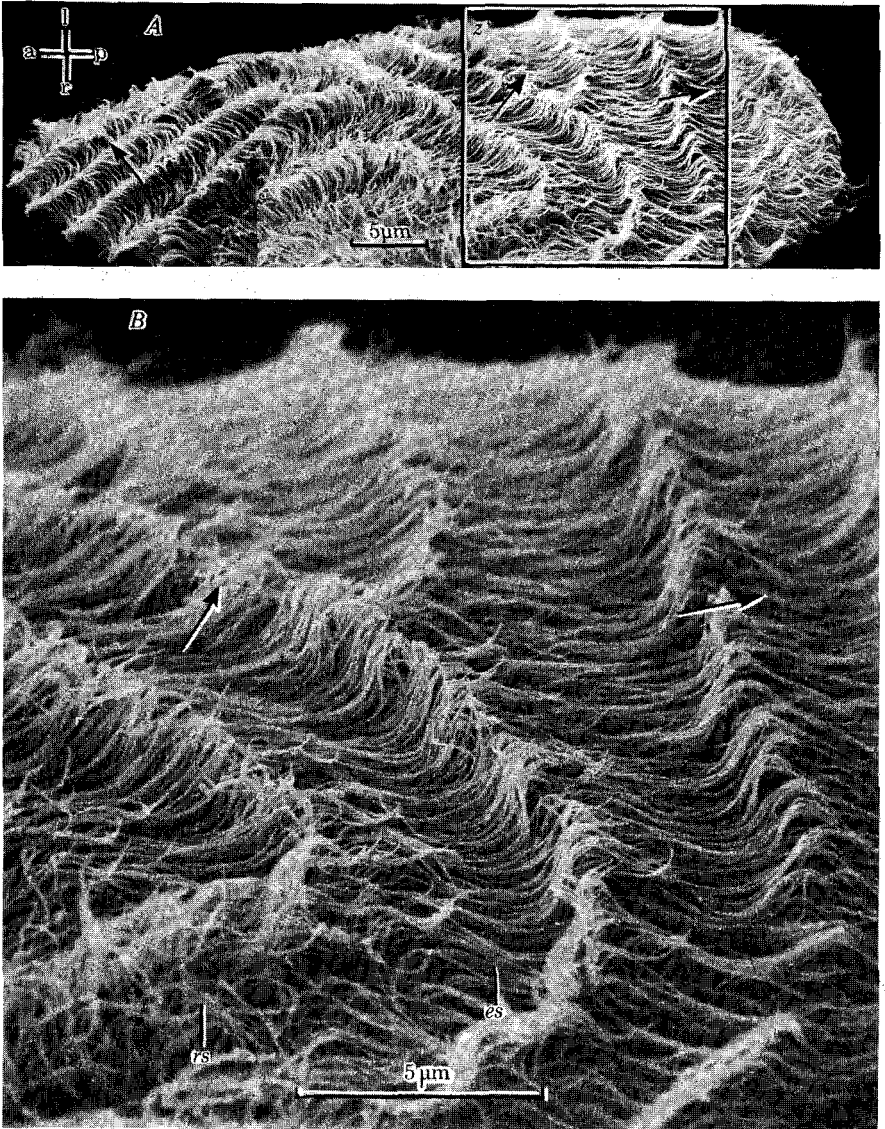


Figure 14 A scanning electron micrograph following rapid fixation of the ciliated protozoan *Opalina* (from Tamm & Horridge 1970). As in the preceding figure, the in vivo metachronal wave orientation is reflected in the pattern over the fixed specimen. Arrows indicate the directions of the metachronal wave. The key difference between the two specimens is that this figure is limited to all or part of a single cell. (We are indebted to Dr. S. L. Tamm for this photograph.)

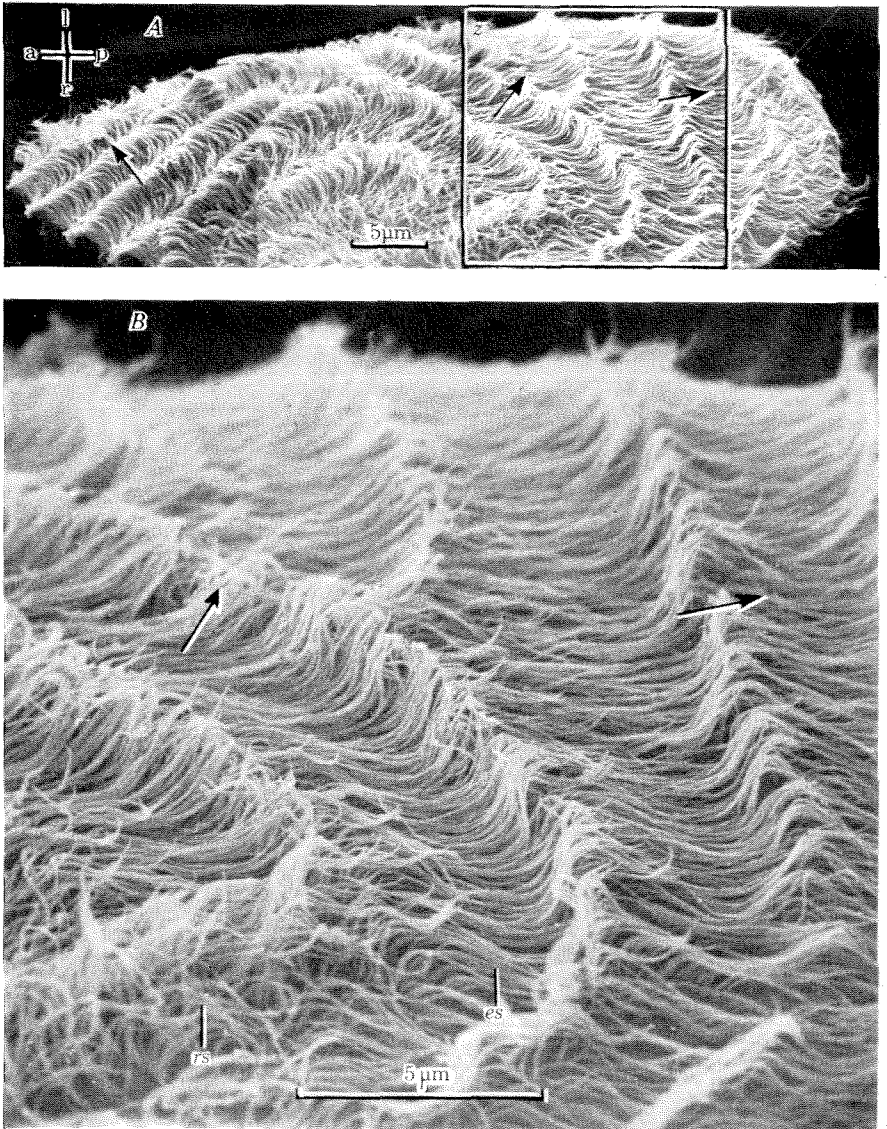


Figure 14 A scanning electron micrograph following rapid fixation of the ciliated protozoan *Opalina* (from Tamm & Horridge 1970). As in the preceding figure, the in vivo metachronal wave orientation is reflected in the pattern over the fixed specimen. Arrows indicate the directions of the metachronal wave. The key difference between the two specimens is that this figure is limited to all or part of a single cell. (We are indebted to Dr. S. L. Tamm for this photograph.)

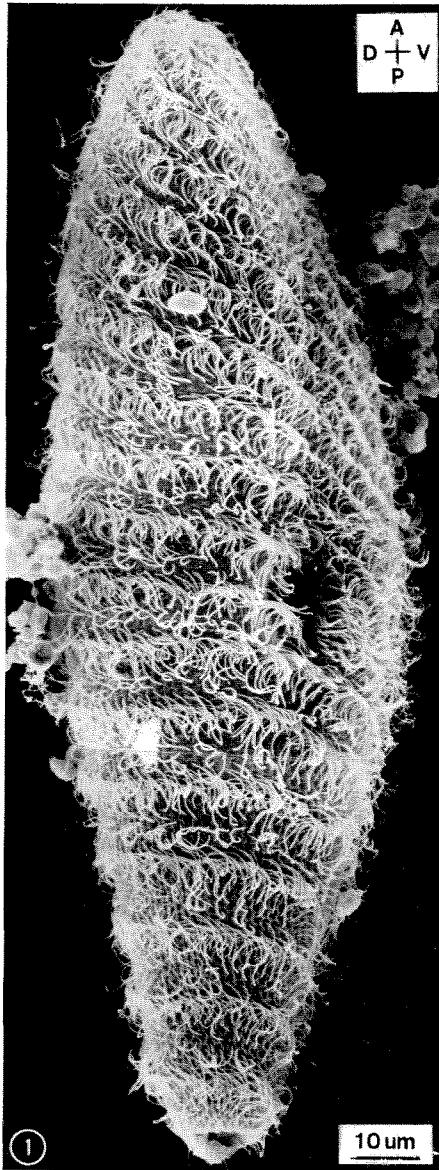
















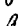
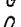


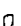






Figure 15 A scanning electron micrograph following rapid fixation of the ciliated protozoan *Paramecium* (from Tamm 1972). The metachrony of this specimen is dexioplectic and/or antiplectic. A-P, anterior-posterior axis; D-V, dorsal-ventral sides. (We are indebted to Dr. S. L. Tamm for this photograph.)

In the following sections we confine ourselves to the hydromechanics of ciliary systems. We would, however, be remiss in not mentioning the important work in which attempts have been made to recover the internal motive force for ciliary beat patterns by working backwards from the known motion, the hydrodynamic forces, and the presumed elastic structure of the cilia (Holwill 1966a, Harris 1961, Sleight & Holwill 1969, Rikmenspoel & Sleight 1970, and Rikmenspoel 1975). Hopefully such analyses will make contact in the future with the electron-microscopy studies

Table 6 Eukaryote propulsion by cilia

Eukaryote	Body		Cilia	
	Length (B) (μm) \times width (μm)	Shape	Cilia length l (μm)	No. cilia/ μm^2 or distribution
<i>Balantidium</i> entozoon	106 \times 55.6			
<i>Coleps</i> hirtus	66 \times 30			
<i>Colpidium</i> sp.	79.1 \times 38.6			
<i>Condylostoma</i> patens	371 \times 102			
<i>Didinium</i> nasutum	126 \times 87			2 circular rows
<i>Euplotes</i> patella ^a	202 \times 124			
<i>Frontonia</i> sp.	378 \times 213			
<i>Halteria</i> grandinella ^a	60 \times 50			
<i>Kerona</i> polyporum ^a	107 \times 64			6 rows cirri
<i>Metopides</i> sp.	115 \times 33			
<i>Nyototherus</i> cordiformis	139 \times 97.2			
<i>Opalina</i> ranarum	350 \times 112		15	1.0
<i>Ophryoglena</i> sp.	250 \times 92.8			
<i>Opisthonecta</i> henneg ^a	126 \times 75			
<i>Paramecium</i> aurelia	125 \times 31			
<i>P. bursaria</i>	126 \times 57			
<i>P. calkinsii</i>	120 \times 44			
<i>P. caudatum</i>	242 \times 48		12	0.5
<i>P. marinum</i>	115 \times 49			
<i>P. multimicronucleatum</i>	251 \times 62			
<i>Prorodon</i> teres	175 \times 160			
<i>Spirostomum</i> ambiguum ^a	1045 \times 95		8.2	
<i>S. polymorphus</i> ^a	208 \times 15.2		27.5	3.5 μm long. separation
<i>Stylonichia</i> sp. ^a	167 \times 86			
<i>Tetrahymena</i> pyriformis	55.7 \times 20		7	17-23 columns
<i>Tillina</i> magna	162 \times 82			
<i>Urocentrum</i> turbo	90 \times 60			2 circ. rows
<i>Uroleptus</i> piscis ^a	203 \times 52			
<i>U. rattulus</i> ^a				
<i>Uronema</i> sp.	40 \times 16			

^a Has undulating membrane and/or membranelles

of the internal structure of cilia, particularly those of Warner & Satir (1974) and Warner (1974).

The fluid mechanics of ciliary systems is clearly quite complex and most of the detailed and quantitative analyses have been based on simplifying assumptions concerning the interaction of the cilia and the fluid. Most of these studies have concentrated on what we shall term local fluid/cilia interaction models; for these purposes most authors have considered an infinite flat surface upon which the cilia

Table 6 Continued

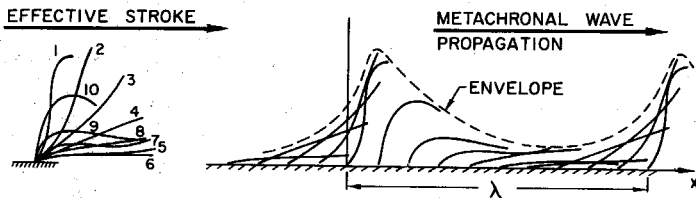
Cilia		Organism				
Metachrony	Wavelength λ (μm)	Cilia beat freq. (Hz)	U/B	U/c	Condition	References
	11.6					149
dxioplectic	10		10.4			47
dxioplectic			2.8		20°C	149
			3.7			47, 149
			6.2			47
			4.3		21.5°C	47
			8.9			47
			4.3			47
dxioplectic	17.1		3.1			47, 149
dxioplectic	26.6					149
symplectic		4				47, 194
dxioplectic	11.4		16			149, 161
dxioplectic		10	9.5			119, 149
			16		21°C	47
			7.9		25°C	47, 48
			8.3			48
	12	29	10.9			48, 149, 199, 200
	10.8		8.1		19°C	47, 48
			11.3			48, 210
			6.1			47
antiplectic	8.5	30	0.78			47, 53
dxioplectic	13	33	4.6	1.26	20-22°C	47, 194, 203
	25.5	59	2.8		22°C	47, 146
dxioplectic	16.2	20	8.1		20°C	149, 162, 231
			12.3			47, 149
			7.8		28.5°C	47
			2.4		22°C	47
					21°C	47
						47

motions are spatially and temporally periodic so as to form metachronal waves. The manner in which such solutions should be applied to finite, ciliated organisms is not entirely obvious; we return to this later. For the present, we discuss the two principal kinds of local fluid/cilia interaction models, the so-called envelope and sublayer models.

5.2 The Envelope Model

The envelope model assumes that the cilia are sufficiently closely packed together, as in the case of *Opalina* in Figure 14, so that the fluid effectively experiences an oscillating material surface. This envelope is commonly assumed to be impenetrable and the motion of each "particle" on the surface is assumed to be roughly equivalent to the locus of the tip of an individual cilium. An analysis of the low-Reynolds-number flow due to such an oscillating sheet was made by Taylor (1951) as a rough two-dimensional model for flagellar propulsion; thus Taylor only pursued the solution in which the "particles" had motions normal to the plane of the surface. Subsequently in a short note Tuck (1968) delineated the nature of the solution in which the oscillatory motions were purely tangential to the surface. Since then, solutions of a more general kind with oscillatory particle motions or ciliary loci of more general form have been produced by Reynolds (1965), Blake (1971b), and Brennen (1974). Consider an arbitrary elliptical form for the ciliary tip locus

OPALINA, SYMPLECTIC METACHRONISM



PARAMECIUM, ANTIPLECTIC METACHRONISM (APPROXIMATION)

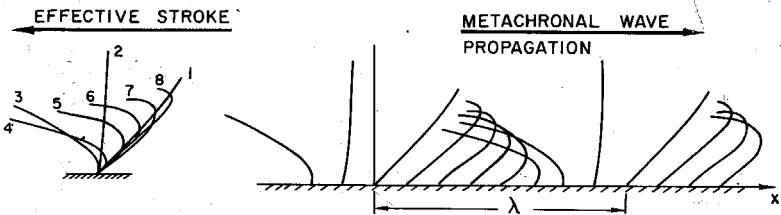


Figure 16 Approximate beat patterns for *Opalina* and *Paramecium* with the positions of an individual cilium at equal intervals in time on the left and the positions of an array of cilia at a given time on the right, showing the symplectic metachronism of *Opalina* and an antiplectic approximation to the metachronism of *Paramecium*.

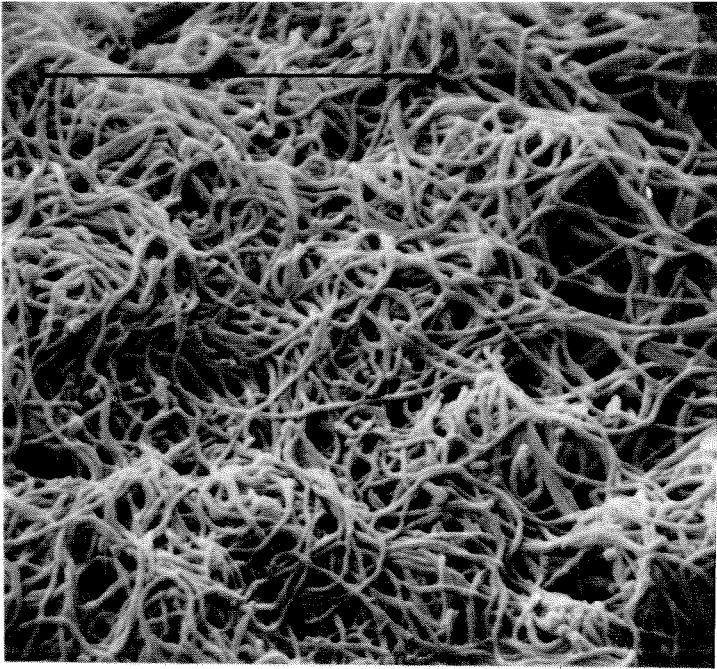


Figure 17 A scanning electron micrograph of the mucociliary epithelium of the olfactory surface of the frog. These cilia operate with no apparent metachrony, and the resulting random motion serves to stir and mix rather than propel the ambient fluid. Accordingly, they may affect transmembrane transport, an important consideration in any chemosensitivity analysis. The scale bar is 10 μm . (We are indebted to Dr. P. P. C. Graziadei for this photograph.)

(Figure 18) in which the tip performs a simple harmonic motion of amplitude h_s tangential to the surface and a simple harmonic motion of amplitude h_n normal to the surface. These deflections of frequency ω have a linear phase shift in the s direction along the surface so as to produce a metachronal wave of velocity, c , and wavelength, λ ($k = 2\pi/\lambda$), travelling in the positive s direction. The mean position of the material surface (and thus of the ciliate) is fixed in this frame of reference. Far from the envelope these oscillatory motions produce a rectilinear translation of the fluid tangential to the sheet whose magnitude in the positive s direction we shall denote by U . If at any point, s , the motion tangential to the surface leads the motion normal to the surface by a phase angle $(\theta - \pi/2)$ and we define a parameter $K = (h_s^2 - h_n^2)/(h_s^2 + h_n^2)$, then the various cilia loci that are so described are indicated diagrammatically in Figure 18. Note that $K = -1$ corresponds to Taylor's (1951) solution, whereas $K = +1$ corresponds to Tuck's (1968) solution. Brennen (1974) has shown that, provided the amplitudes h_s and h_n are small compared with the

wavelength λ and the Reynolds number $Re = \omega/k^2\nu$ is small, the translation velocity, U , is given by

$$\frac{U}{c} = \frac{1}{2}k^2(h_s^2 + h_n^2) \left[\frac{(\beta + 1)}{2\beta} (1 - K^2)^{1/2} \cos \theta - \frac{(\beta - 1)}{2\beta} - K \right] \quad (28)$$

where

$$\beta = \left\{ \frac{1}{2}[(1 + Re^2)^{1/2} + 1] \right\}^{1/2}.$$

Notice that this steady translation is quadratic in the nondimensional amplitudes kh_s , and kh_n ; since these are assumed small, the velocity U is much smaller than the oscillatory velocities produced by motion of the envelope, which are first-order in kh_s and kh_n and which, incidentally, decay like e^{-kn} with normal distance, n , away

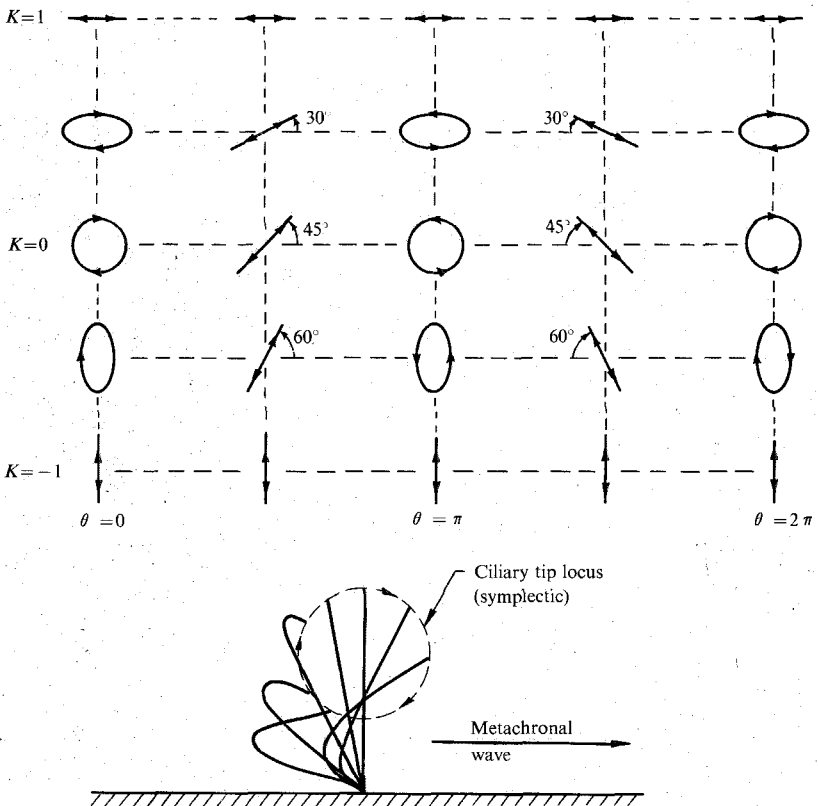


Figure 18 Variations of arbitrary elliptical ciliary tip loci with the parameters K and θ . The figure is correlated with the cell surface horizontal, the fluid above it and the metachronal waves travelling to the right. An example of a ciliary tip locus (symplectic) is indicated in the lower part of the figure.

from the envelope. The translation, U , arises from two different quadratic combinations of first-order oscillatory terms. The first and most important is in the quadratic term of the Taylor series expansion through which the velocity conditions on the envelope are satisfied. The second quadratic term is $O(\text{Re})$ smaller and arises from the inertia terms in the Navier-Stokes equations. The latter disappears, therefore, when $\text{Re} \rightarrow 0$ and then

$$\frac{U}{c} \rightarrow \frac{1}{2}k^2(h_s^2 + h_n^2)[(1 - K^2)^{1/2} \cos \theta - K], \tag{29}$$

which is in agreement with Blake's (1971b) results. The variation of the propulsion velocity, U , with the (K, θ) parameters was investigated by Brennen and is shown in Figure 19 in which contours of constant $U/c k^2(h_s^2 + h_n^2)$ are plotted. Notice that this exhibits two optimum forms for the ciliary locus. When $K = -1/\sqrt{2}$ and $\theta = 0$ a maximum propulsive velocity of $ck(h_s^2 + h_n^2)/\sqrt{2}$ is achieved in the positive s direction, a situation that corresponds to symplectic metachronal propulsion. A simple Galilean transformation to bring the fluid at infinity to rest models a cilium travelling in a direction opposite to the direction of wave propagation. On the other hand, maximum antiplectic propulsion of the same magnitude can equally well be achieved with a ciliary tip locus for which $K = +1/\sqrt{2}$, $\theta = \pi$ (see Figure 18). The energy expenditure per unit surface area, \dot{E} , for these motions is simply given by $\mu c^2 k^3(h_s^2 + h_n^2)$. It follows that the above optima are also the most efficient means of propulsion in terms of propulsive velocity per unit energy expenditure per unit area. Finally, we note that calculations based on the expression (28) for nonzero

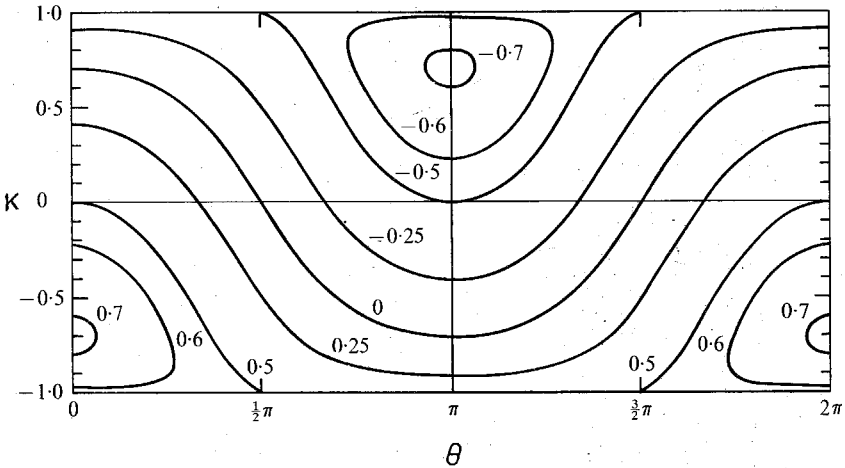


Figure 19 Variation of the dimensionless propulsive velocity $U/c k^2(h_s^2 + h_n^2)$ with the ciliary tip locus parameters K and θ according to the envelope model result (29). Contours are shown for various labelled values of $U/c k^2(h_s^2 + h_n^2)$; the figure should be used in conjunction with Figure 18.

Reynolds number indicate that even when Re is of order unity, the contours are little changed from those of Figure 19 (Brennen 1974).

Envelope models of this kind have been applied to a wide variety of physiological situations. Blake (1971b) and Brennen (1974, 1975) considered their application to the locomotion of ciliated microorganisms. Katz (1972) and Shack & Lardner (1972) used the method to model the propulsion of fluid in the ciliated tubes of mammalian reproductive systems, both female and male (see also Blake 1973b). In this regard considerable attention has been given to the role of the cilia in the mammalian oviduct in propelling the ovum. Ross (1971) has also used an envelope model to study the propulsion of mucus by the ciliated epithelium of the trachea. Such analyses have much in common with peristaltic pumping (Jaffrin & Shapiro 1971) where the "envelope" is a real material surface; in this case, considerations of and conditions upon the extensibility of the envelope are often imposed.

Apart from other more general problems to be discussed below, one of the major difficulties in comparing results from envelope model analyses with observations is that most of these analyses are limited to amplitudes h_s and h_n that are small compared with the metachronal wavelength, λ ; that is, kh_s and kh_n are small. On

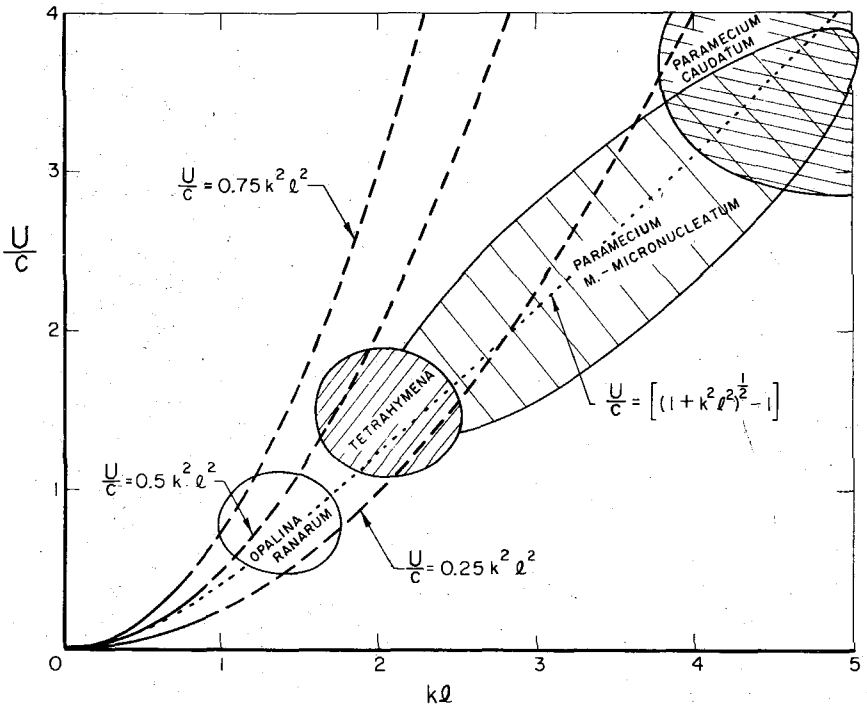


Figure 20 Comparison of the propulsive velocity of some ciliates (data given by areas denoting the scatter in the available information) with extrapolated predictions of envelope theories of the form $U/c \propto k^2 \lambda^2$.

the other hand, as illustrated by the values in Table 6, most ciliary systems appear to operate with values of kh_s or kh_n that are of order one or greater. This point is exemplified by the data presented in Figure 20, where values of U/c are compared with kl , l being the cilia length; for purposes of comparison with the expression (29) and Figure 20 we may note that for many real ciliary beat patterns

$$l^2 \approx 4(h_s^2 + h_n^2).$$

Blake (1971b) has done some preliminary envelope analysis for larger amplitudes by evaluating higher-order terms in kh_s , kh_n . But further nonlinear analyses, which also incorporate higher-order harmonics in time in order to model the differences in the speeds of the "effective" and "recovery" strokes, are probably necessary before a conclusive evaluation of the utility of envelope models can be made.

5.3 Sublayer Models

A second distinct set of models has been proposed and developed for ciliary systems. These models concentrate on the interactions between individual cilia with the surrounding fluid and hence deal specifically with the flow among the cilia. For this reason they have been termed sublayer models. Blake (1972) first proposed such an analysis for the flow created by a regular array of cilia beating metachronously on an infinite plane wall.

By considering the relative motion between an element of a cilium and the surrounding fluid, sublayer models seek to establish the incremental force (or stokeslet strength) on each and every cilium element through use of resistive-force theory. The entire flow field, denoted by its velocity $\mathbf{q}(\mathbf{x})$ where \mathbf{x} is a position vector, is then considered as having been created by this distribution of stokeslets and can be formally represented as an integral of the velocities induced at each point by each cilium element. Since these slender bodies operate close to a wall, the effect of the image system of singularities should also be included in order to satisfy a no-slip condition at that boundary. This has important consequences for ciliary propulsion because of the different forms of image systems for stokeslets oriented normal and tangential to the wall, as discussed in section 2.4. Since the far-field for normal stokeslets decays more rapidly (like r^{-3}) than that of tangential stokeslets (like r^{-2}), it follows that the tangential motion of the ciliary elements is of much greater consequence than the normal motion.

The fluid-mechanical problem is completely defined when the relative motion between an elemental length of cilium at a position \mathbf{x}_0 and its surrounding fluid is formulated in terms of a known cilium motion due to a specified beat pattern and the fluid velocity, $\mathbf{q}(\mathbf{x}_0)$. There is, however, a difficulty here because the model presupposes that after a Galilean transformation utilizing $\mathbf{q}(\mathbf{x}_0)$ the element is translating as though in fluid at rest far from the element. This implies that the methods developed up to the present time must be limited to situations in which the cilia are sufficiently widely spaced so that the local flow field around one cilium does not extend to the neighboring cilia. One is left with the impression that such difficulties are not entirely resolved in the existing literature. Indeed, Blake & Sleight (1974) have pointed out that desirable improvements to the present sublayer models

could be provided by studies of the translation of slender bodies in the presence of other similar bodies.

The above description suggests an iterative scheme that begins with a best guess for $\mathbf{q}(\mathbf{x})$ and proceeds through evaluation of the stokeslets to the calculation of a "new" velocity field $\mathbf{q}(\mathbf{x})$. Such iterative methods have been used by Keller, Wu & Brennen (1975). Alternatively the problem may be put in the form of an integral equation for $\mathbf{q}(\mathbf{x})$ as originally demonstrated by Blake (1972).

In his sublayer analyses Blake (1972) included only a *steady* or time-averaged velocity of the fluid tangential to the wall, u , in his calculation of the stokeslet strength and obtained the steady velocity profile $u(x_3)$ (x_3 being the coordinate normal to the wall) that results from his solution of the integral equation. Keller, Wu & Brennen (1975) pointed out, however, that since oscillatory velocities of comparable and greater magnitude are created by the cilia motions these should be included in evaluation of the forces on individual cilium elements. They used a method somewhat different from that of Blake in which these forces are smoothed out to form a continuous body force field within the cilia layer and their solution is achieved by solving the Stokes equations in this layer with these body force terms included. The resulting iterative solution yields a velocity profile not only for the steady velocities but also for the oscillatory velocities both normal and tangential to the wall.

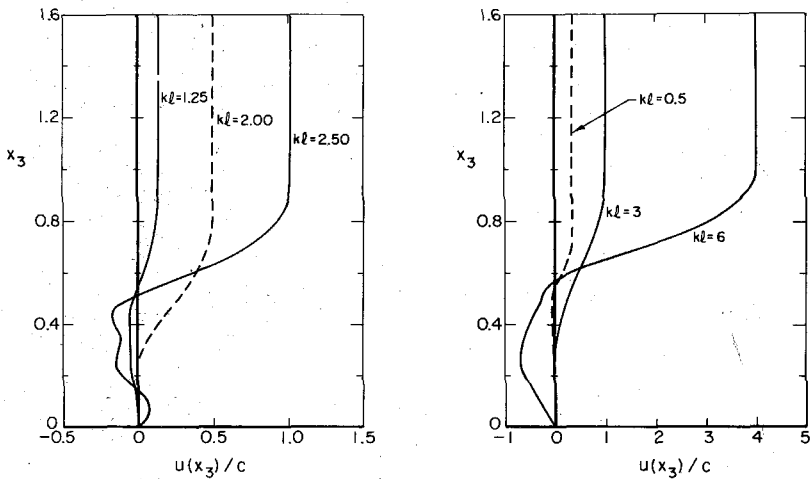


Figure 21 Mean tangential velocity profiles within the ciliary array (the normal coordinate, x_3 , has been nondimensionalized by the cilia length l) for *Opalina* (left) and *Paramecium* (right) by using the planar beat forms of Figure 16. The dashed lines (Blake 1972) neglect the oscillatory velocity interactions of the cilia and were computed for cilia spaced at intervals d_1, d_2 on the cell surface, where $k^2 d_1 d_2$ was assumed to be 0.04 for *Opalina* and 0.00025 for *Paramecium*. The solid lines (Keller, Wu & Brennen 1975) include oscillatory velocities and are computed for values of $k^2 d_1 d_2$ of 0.082 and 1.3, values apparently more consistent with the observed cilia distributions.

The solutions are all obtained in a frame fixed in the organism so that $u(\infty)$ is the propulsive velocity of the ciliary system. Indeed a particular feature of all the present infinite-sheet sublayer models is that $u(x_3)$ remains constant beyond the maximum extent of the ciliary tips; we return to this point later. The majority of existing solutions are also for purely planar cilia beat patterns and for purely symplectic or antiplectic metachronism. As observed earlier, virtually all beat patterns contain to some greater or lesser degree displacements in all three coordinate directions and have metachronal patterns that deviate toward the diaplectic. Velocity profiles derived by Blake (1972) and Keller, Wu & Brennen (1975) for *Opalina* and *Paramecium* are shown in Figure 21; these are based on the planar beat patterns of Figure 16 and the assumption of symplectic and antiplectic metachronism for these two organisms, respectively. In both cases there are practical difficulties because the cilia of *Opalina* are too densely packed (see Figure 14) for one to have confidence in the sublayer model as presently constituted, and in the case of *Paramecium* because the metachronism is diaplectic and the beat three-dimensional (see above). The latter point was later rectified by Blake (1974a) who incorporated three-dimensionality in a sublayer model for *Paramecium*.

Apart from the individual imperfections of the two local fluid/cilia interaction models mentioned above, there are further difficulties in applying either to real physiological systems. We confine ourselves here to discussion of two of the principal difficulties to which some attention and thought has been given.

5.4 Ciliated Organisms

Apart from the infinite-sheet geometries discussed above, several attempts have been made to apply these models to finite organisms. In the first solution of this kind Blake (1971a), extending earlier work by Lighthill (1952), approximated small-amplitude travelling waves on a spherical body by combining two spherical-harmonic functions whose orders differed by one. This envelope model is rather restrictive in terms of the permitted variation of wave form and amplitude and it approximates travelling waves only near the maximum width of the body.

Subsequently Brennen (1974, 1975) has pointed out that the flow around most ciliated organisms for which the metachronal wavelength is small compared with overall dimensions will be comprised of two parts: (a) a relatively thin oscillatory boundary layer within which the oscillatory motions created by the cilia will decay rather rapidly with distance from the surface and (b) an outer steady Stokes flow around the organism. The problem is then to find some way of matching a local fluid/cilia interaction model within the boundary layer to the so-called complementary Stokes flow outside the boundary layer. For self-propelling organisms this complementary Stokes flow and the velocity of propulsion can only be obtained explicitly after application of the condition of zero total force on the organism; the velocity field far from the organism in this case probably cannot be like a stokeslet since the self-propelling organism exerts no net steady force on the fluid. It must be like a Stokes doublet or higher order. In this regard it is of interest to relate that some recent flow-visualization experiments with minute polystyrene tracer particles suggest that it is *not* like a Stokes doublet but more like that of a

potential doublet (Keller & Wu 1976). Such a flow has less dissipation of energy than the Stokes doublet, which suggests that the ciliary system, at least in the organism observed, has been optimized to the extent of producing a complementary Stokes flow that does not contain a Stokes-doublet component. On the other hand, if the organism is pinned down, the complementary Stokes flow will be like that of a stokeslet in the far field and the thrust produced by the restrained organism can be computed. Brennen (1974, 1975) has applied such a matching technique to the propulsion of spherical and ellipsoidal ciliates using an envelope model for the local fluid/cilia interaction, and Blake (1973a) has also considered the effect of a finite cell body on results obtained for infinite-sheet models.

One particular feature of Brennen's results (1974, 1975) is that they allow evaluation of the thrust, T , that a restrained organism can produce. [With regard to this it is worth noting, as Taylor (1951) did, that there is zero net thrust in the infinite-sheet solutions.] Typical values from an envelope model are shown in Figure 22 for direct comparison with Figure 19. Note that the ciliary beat patterns for optimum thrust on restrained organisms differ from those for optimum rectilinear propulsive velocity. This raises questions, which will not otherwise be discussed here, of whether a large starting (or turning) thrust or an optimum steady propulsive velocity is of greater importance for individual species.

Recently some attempts have been made to measure the actual velocity profiles near the surface of ciliated microorganisms. Cheung & Winet (1975) report on some such measurements on *Spirostomum* using minute polystyrene tracer particles. One would hope that further quantitative data for other physiological situations will be obtained in order to allow detailed evaluation of the theoretical models. The mean velocity profiles of Cheung & Winet (1975) are shown in Figure 23. A particular

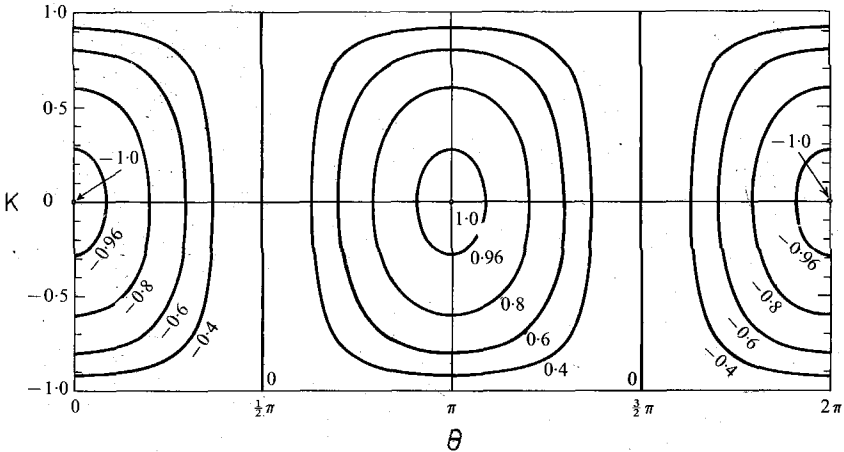


Figure 22 Typical contours of the nondimensional thrust, $3T/4\pi\mu k^2(h_s^2 + h_n^2)Ac$, where T is thrust developed by a restrained ciliate of typical dimension $2A$, according to an envelope model for the fluid/cilia interaction (Brennen 1975). For comparison with Figures 18 and 19.

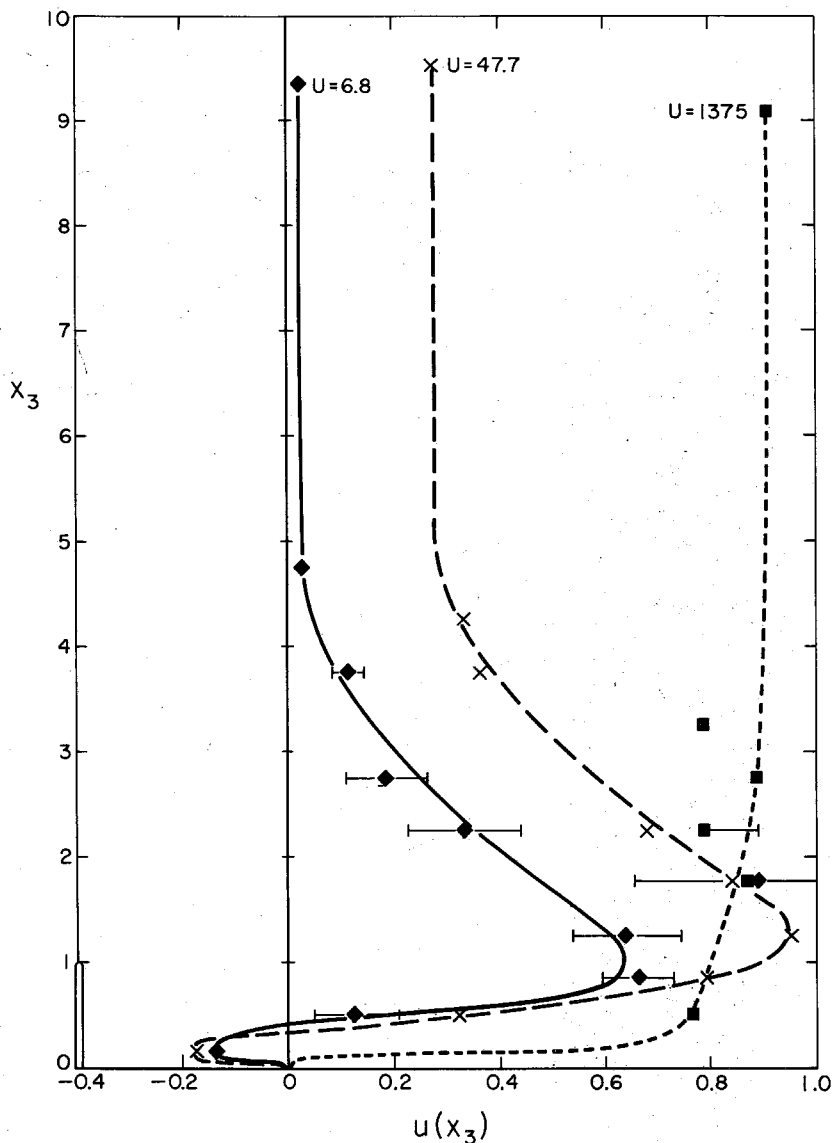


Figure 23 Measured mean tangential velocity profiles for a swimming *Spirostomum* for different swimming speeds U (in $\mu\text{m}/\text{sec}$) as indicated [from Cheung & Winet (1975), who observed polystyrene tracer particle motions]. The normal coordinate x_3 is given in cilia lengths and the horizontal velocity axis has been nondimensionalized by dividing by the fastest tracer particle value for each profile. Effective stroke toward the right.

feature of these results concerns the variation of the mean tangential velocity with distance, x_3 , from the surface (here normalized with respect to cilia length) for the larger values of x_3 . The corresponding envelope model for an infinite sheet would suggest that the velocity approaches its asymptotic value within a value of x_3 of about 3; the sublayer model for an infinite sheet has no variation beyond $x_3 = 1$. Thus it would seem that one is measuring the complementary Stokes flow at the higher values of x_3 ; hence the aforementioned need to understand the interaction between this predominantly steady flow and the more localized and unsteady interaction between the cilia and the fluid. In this context studies of the propulsion of ciliates in tubes can yield important information (Winet 1973).

5.5 *Internal Flows and the Propulsion of Mucus*

It appears that the primary difficulty regarding internal flows (and a number of external flows: Jahn et al 1965, Jahn & Hendrix 1969, Winet & Jones 1975) in organs with ciliated epithelia is that the fluid usually is non-Newtonian. This fluid virtually always consists of mucus or some other association of glycoproteins. Such systems are called *mucoiliary systems*. When the concentration of these long-chain polymers in the colloidal system is greater than about 1% (wt vol⁻¹), the system invariably displays significant viscoelastic, shear-thinning, or thixotropic effects. At higher concentrations gel particles and eventually gel networks form. At all mucin concentrations up to and including the ones that produce gelation—the network-formation process—liquefaction (gel → sol transformation) will occur under applied stress (see Frey-Wyssling 1952; Eliezer 1974; Litt 1970; Hwang, Litt & Forsman 1969; and others).

The propulsion of mucus in mammalian trachea is one such situation that appears to be dominated by viscoelastic effects. The conventional view is that a blanket of highly viscoelastic mucus lining the airway is propelled by cilia that are surrounded by a much less viscous fluid (serous fluid). The cilia appear to move the blanket by contacting it only during the effective stroke (Cheung & Jahn 1975). Experiments by Sadé et al (1970) have indicated that the propulsion of mucus is quite sensitive to the form and state of the mucus, with optimum propulsion occurring when the concentration of glycoprotein is close to that of the sol → gel transformation. Ross & Corrsin (1974) constructed a theoretical two-fluid-layer model (inner serous-fluid layer and outer viscoelastic blanket of mucus) for mucus transport employing an envelope model for the cilia/serous fluid interaction. Their calculations indicate that propulsion is enhanced when the mucus is fairly rigid and when the ciliary tip loci have predominantly horizontal motions. Blake (1975) has also applied his sublayer method to model the interaction of the cilia and the serous fluid (see also Miller 1969 and Barton & Raynor 1967) and the subsequent propulsion of a solid slab representing the mucus blanket; he also gives a qualitative discussion of the effects of the elasticity of the slab.

However, the observation by Cheung & Jahn (1975) of more direct mechanical propulsion of the mucus blanket appears to require a reevaluation of the fluid mechanics of tracheal mucus propulsion. If the cilia penetrate the mucus only during the effective stroke, this provides a much more direct mechanism for mucus pro-

pulsion. Furthermore, such a mechanism would not require any particular organization of the metachrony of the cilia, unlike most of the fluid-mechanical models. Indeed, some confirmation of this direct-contact mechanism is provided by the fact that propulsion seems to take place in the absence of organized metachronism (Cheung & Jahn 1975), which is often hard to observe in tracheal cilia. The observations suggest that the cilia attached to each ciliated cell (which are usually interspersed with secretion cells) beat in synchrony but that any relationship between the phase of the cilia on different cells is not readily apparent. It should be noted, however, that the tissue utilized for this study was observed *in vitro* (i.e. removed from its site in the organism and macerated to create a layer thin enough for observation on a thin slide preparation), and *in vivo* influences on ciliary motion such as the nervous effect described by Murakami & Takahashi (1975) could not have been taken into account. In any case a reexamination of the fluid mechanics of tracheal mucociliary propulsion should also show awareness that both the mucus blanket and the distribution of ciliated cells on the epithelium can be quite nonuniform.

In mucociliary systems where mucus is an incidental component of the propelled object, e.g. the mammalian oviduct in which ova and perhaps spermatozoa are the primary objects of ciliary activity, the role of mucus is not clear. It has long been assumed, for example, that mucus acts as a lubricant for the transport of ova down the isthmus of the oviduct. No quantitative test of this assumption appears to have been conducted *in situ*. A model system utilized recently for measuring the lubrication effect (Winet 1976) consists of a ciliated spheroid swimming down a mucin-filled tube. Observations of this system indicate not only a lubrication effect for small clearances but also an optimized drag reduction effect at larger clearances. Although we have concentrated here on tracheal mucus flows, we should mention in closing that there are many other internal flows in ciliated tubes such as the ductus efferentes and the oviduct for which some modification of an infinite-sheet model may suffice (e.g. Blake 1975). Some of the characteristics of internal ciliary systems have been collected in Table 7. However, neither sufficiently detailed observations nor complete quantitative information are presently available to allow confident examination of most of these ciliary systems.

6 CONCLUDING REMARKS

In closing we should emphasize again that, although we have concentrated in this review on the fluid mechanics of cilia and flagella, a complete understanding of the life functions of these biological systems requires much more than fluid mechanics. At the same time, fluid mechanics is an integral component of any quantitative analysis for the contraction processes and indicates where ciliation and flagellation give selective advantages to organisms not only in terms of their ability to propel fluids but also in terms of biosynthesis and concentration. Indeed, the ubiquity of these systems as indicated by Table 1 would itself be a worthy study by comparative physiologists.

We have thus attempted to give an overview of the fluid mechanics of these

biological slender bodies. It should be clear that the subject is still in a developmental stage and much remains to be done. One expects to see further developments in the basic fluid mechanics of slender bodies at low Reynolds numbers, especially when these operate close to a large "cell" body. Furthermore, the present understanding of the fluid mechanics of ciliary systems is still rather limited and we have tried to indicate that there are many other ciliary systems that have not yet received attention from a fluid-mechanical point of view. But in conclusion we must stress that a multidisciplinary approach is very necessary for any assessment of the fluid-mechanical models and, consequently, for a fuller understanding of cilia and flagella and the life functions they attend.

ACKNOWLEDGMENTS

The authors gratefully acknowledge support from the National Science Foundation under Grants ENG 74-23008 A01 and AEN 72-03586 A01 and from the Office of Naval Research under Contract N 00014-76-C-0157 during the preparation of this paper. We should also like to thank Professor T. Y. Wu, Professor C. J. Brokaw, Dr. A. T. Chwang, and Mr. R. E. Johnson for their assistance as well as those who permitted us to use their photographs.

Literature Cited

- Adler, J. 1976. The sensing of chemicals by bacteria. *Sci. Am.* 234:40-47
- Aiello, E., Sleight, M. A. 1972. The metachronal wave of lateral cilia of *Mytilus edulis*. *J. Cell Biol.* 54:493-506
- Anderson, R. A. 1975. Formation of the bacterial flagellar bundle. See Ref. 234, pp. 45-56
- Andrew, W. 1959. *Textbook of Comparative Histology*. New York: Oxford Univ. Press. 652 pp.
- Austin, C. R. 1965. *Fertilization*, pp. 34-35. Englewood Cliffs, NJ: Prentice-Hall
- Baccetti, B. et al 1975. Motility patterns in sperms with different tail structure. In *The Functional Anatomy of the Spermatozoon*, ed. B. A. Afzelius, pp. 141-50. Elmsford, NY: Pergamon
- Barber, V. C. 1974. Cilia in sense organs. See Ref. 199, pp. 403-36
- Barton, C., Raynor, S. 1967. Analytical investigation of cilia-induced mucous flow. *Bull. Math. Biophys.* 29:419-28
- Batchelor, G. K. 1970a. Slender body theory for particles of arbitrary cross-section in Stokes flow. *J. Fluid Mech.* 44:419-40
- Batchelor, G. K. 1970b. Stress system in a suspension of force-free particles. *J. Fluid Mech.* 41:545-70
- Beck, L. T., Boots, I. R. 1974. The comparative anatomy, histology and morphology of the mammalian oviduct. In *The Oviduct and Its Functions*, ed. A. D. Johnson, C. E. Foley, pp. 1-52. New York: Academic
- Berg, H. C. 1974. Dynamic properties of bacterial flagellar motors. *Nature* 249:77-79
- Berg, H. C. 1975. Bacterial movement. See Ref. 234, Vol. I, pp. 1-11
- Berg, H. C., Anderson, R. A. 1973. Bacteria swim by rotating their flagellar filaments. *Nature* 245:380-82
- Bharier, M. A., Rittenberg, S. C. 1971. Chemistry of axial filaments of *Treponema zuelzeriae*. *J. Bacteriol.* 105:422-29
- Black, J., Korostoff, E. 1974. Strain-related potentials in living bone. *Ann. NY Acad. Sci.* 238:95-120
- Blake, J. R. 1971a. A spherical envelope approach to ciliary propulsion. *J. Fluid Mech.* 46:199-208
- Blake, J. R. 1971b. Infinite models for ciliary propulsion. *J. Fluid Mech.* 49:209-22
- Blake, J. R. 1971c. A note on the image system for a Stokeslet in a no-slip boundary. *Proc. Cambridge Philos. Soc.* 70:303-10
- Blake, J. R. 1972. A model for the micro-structure in ciliated organisms. *J. Fluid Mech.* 55:1-23
- Blake, J. R. 1973a. A finite model for ciliated microorganisms. *J. Biomech.* 6:133-40

22. Blake, J. R. 1973b. Flow in tubules due to ciliary activity. *Bull. Math. Biol.* 35: 513-23
23. Blake, J. R. 1974a. Hydrodynamic calculations on the movements of cilia and flagella. Part I. *Paramecium*. *J. Theor. Biol.* 45: 183-203
24. Blake, J. R. 1974b. Singularities of viscous flow. Part II. Applications to slender body theory. *J. Eng. Math.* 8: 113-24
25. Blake, J. R. 1975. On the movement of mucus in the lung. *J. Biomech.* 8: 179-90
26. Blake, J. R., Chwang, A. T. 1974. Fundamental singularities of viscous flow. Part I. The image systems in the vicinity of a stationary no-slip boundary. *J. Eng. Math.* 8: 23-29
27. Blake, J. R., Sleight, M. A. 1974. Mechanics of ciliary locomotion. *Biol. Rev.* 49: 85-125
28. Borradaile, L. A., Potts, F. A. 1958. *The Invertebrata*. Cambridge: Univ. Press. 795 pp. 3rd ed.
29. Bourne, G. J. 1960. *The Structure and Function of Muscle*, Vol. I, *Structure*. New York: Academic. 472 pp.
30. Boyce, E. C. 1965. Swimming movement of *Eimeria* sp. merozoites. *Progress in Protozoology, 2nd Int. Conf. Protozool.* Abstr. No. 166, p. 152
31. Bradfield, J. R. G., Cater, D. B. 1952. Electron-microscopic evidence on the structure of spirochaetes. *Nature* 169: 944
32. Breed, R. S., Murray, E. G. D., Smith, N. R. 1957. *Bergey's Manual of Determinative Bacteriology*. Baltimore: Williams & Wilkins. 1094 pp.
33. Brennen, C. 1974. An oscillating-boundary-layer theory for ciliary propulsion. *J. Fluid Mech.* 65: 799-824
34. Brennen, C. 1975. Hydromechanics of propulsion for ciliated microorganisms. See Ref. 234, pp. 235-52
35. Brennen, C. 1976. Locomotion of flagellates with mastigonemes. *J. Mechanochem. Cell Motil.* 3: 207-17
36. Brenner, H. 1962. Effect of finite boundaries on the Stokes resistance of an arbitrary particle. *J. Fluid Mech.* 12: 35-48
37. Brenner, R. M. 1969. Renewal of oviduct cilia during the menstrual cycle of the Rhesus monkey. *Fertil. Steril.* 20: 599-611
38. Brinkman, G. E. 1966. Discussion. *Am. Rev. Respir. Dis.*, 93, no. 3, pt. 2: 60
39. Broersma, S. 1960. Viscous force constant for a closed cylinder. *J. Chem. Phys.* 32: 1632-35
40. Brokaw, C. J. 1963. Movement of the flagella of *Polytoma uwella*. *J. Exp. Biol.* 40: 149-56
41. Brokaw, C. J. 1965. Non-sinusoidal bending waves of sperm flagella. *J. Exp. Biol.* 43: 155-69
42. Brokaw, C. J. 1970. Bending moments on free-swimming flagella. *J. Exp. Biol.* 53: 445-64
43. Brokaw, C. J. 1971. Bend propagation by a sliding filament model for flagella. *J. Exp. Biol.* 55: 289-304
44. Brokaw, C. J. 1972. Computer simulation of flagellar movement. *Biophys. J.* 12: 564-86
45. Brokaw, C. J. 1975. Spermatozoan motility: A biophysical survey. *Biol. J. Linn. Soc.* 7: Suppl. 1, pp. 423-39
46. Brokaw, C. J., Gibbons, I. R. 1975. Mechanisms of movement in flagella and cilia. See Ref. 234, Vol. I, pp. 89-132
47. Bullington, W. E. 1925. A study of spiral movement in the ciliate infusoria. *Arch. Protistenkd.* 50: 219-74
48. Bullington, W. E. 1930. A further study of spiraling in the ciliate *Paramecium*, with a note on morphology and taxonomy. *J. Exp. Zool.* 56: 423-51
49. Burgers, J. M. 1938. On the motion of small particles of elongated form suspended in a viscous fluid. *K. Ned. Akad. Wet. Verhand.* 16, no. 4: 113-84
50. Calladine, C. R. 1974. Bacteria can swim without rotating flagellar filaments. *Nature* 249: 385
51. Carson, S., Goldhamer, R., Carpenter, R. 1966. Mucus transport in the respiratory tract. *Am. Rev. Respir. Dis.*, 93, no. 3, pt. 2: 86-92
52. Cheung, A. T. W., Jahn, T. L. 1975. Determination of the movement pattern of the epithelial cilia of rabbit trachea and the clearance mechanism of the tracheal mucus-ciliary clearance system. See Ref. 234, Vol. I, pp. 289-300
53. Cheung, A. T. W., Winet, H. 1975. Flow velocity profile over a ciliated surface. See Ref. 234, Vol. I, pp. 223-34
54. Chwang, A. T. 1975. Hydromechanics of low-Reynolds-number flow. Part 3. Motion of a spheroidal particle in quadratic flows. *J. Fluid Mech.* 72: 17-34
55. Chwang, A. T., Winet, H., Wu, T. Y. 1974. A theoretical mechanism for spirochetal locomotion. *J. Mechanochem. Cell Motil.* 3: 69-76
56. Chwang, A. T., Wu, T. Y. 1971. A note on the helical movement of microorganisms. *Proc. R. Soc. London Ser. B*

- 178: 327-46
57. Chwang, A. T., Wu, T. Y. 1974. Hydro-mechanics of low-Reynolds-number flow. Part 1. Rotation of axisymmetric prolate bodies. *J. Fluid Mech.* 63: 607-22
 58. Chwang, A. T., Wu, T. Y. 1975. Hydro-mechanics of low-Reynolds-number flow. Part 2. Singularity method for Stokes flows. *J. Fluid Mech.* 67: 787-815
 59. Chwang, A. T., Wu, T. Y. 1976. Hydro-mechanics of low-Reynolds-number flow. Part 4. Translation of spheroids. *J. Fluid Mech.* 75: 677-89
 60. Chwang, A. T., Wu, T. Y., Winet, H. 1972. Locomotion of spirilla. *Biophys. J.* 12: 1549-61
 61. Cleveland, L. R., Cleveland, B. T. 1966. The locomotory waves of *Koruga*, *Deltotrychonympha* and *Mixotricha*. *Arch. Protistenkd.* 109: 39-63
 62. Coakley, C. J., Holwill, M. E. J. 1972. Propulsion of microorganisms by three-dimensional flagellar waves. *J. Theor. Biol.* 35: 525-42
 63. Costello, D. P. 1973a. A new theory on the mechanics of ciliary and flagellar motility. I. Supporting observations. *Biol. Bull.* 145: 279-91
 64. Costello, D. P. 1973b. A new theory on the mechanics of ciliary and flagellar motility. II. Theoretical considerations. *Biol. Bull.* 145: 292-309
 65. Cox, P. J., Twigg, G. I. 1974. Leptospiral motility. *Nature* 250: 260-61
 66. Cox, R. G. 1970. The motion of long slender bodies in a viscous fluid. Part 1. General theory. *J. Fluid Mech.* 44: 791-810
 67. Davis, R. E., Worley, J. F. 1973. Spiroplasma: Motile helical microorganism associated with corn stunt disease. *Phytopathology* 63: 403-8
 68. de Mestre, N. J. 1973. Low-Reynolds-number fall of slender cylinders near boundaries. *J. Fluid Mech.* 58: 641-56
 69. de Mestre, N. J., Russel, W. B. 1975. Low-Reynolds number-translation of a slender cylinder near a plane wall. *J. Eng. Math.* 9: 81-91
 70. Denchy, M. A. 1975. The propulsion of non-rotating ram and oyster spermatozoa. *Biol. Reprod.* 13: 17-29
 71. DePamphilis, M. L., Adler, J. 1971. Fine structure and isolation of the hook-basal body complex of flagella from *Escherichia coli* and *Bacillus subtilis*. *J. Bacteriol.* 105: 384-95
 72. Dirksen, E. R., Satir, P. 1972. Ciliary activity in the mouse oviduct as studied by transmission and scanning electron microscopy. *Tissue Cell* 4: 389-404
 73. Doetsch, R. N. 1966. Some speculations accounting for the movement of bacterial flagella. *J. Theor. Biol.* 11: 411-17
 74. Douglas, G. J. 1975. Sliding filaments in sperm flagella. *J. Theor. Biol.* 53: 247-52
 75. Dryl, S. 1975. Local microtubules interaction theory of ciliary and flagellar motion. *Bull. Acad. Polon. Sci. Ser. Sci. Biol.* 23: 339-46
 76. Eliezer, N. 1974. Viscoelastic properties of mucus. *Biorheology* 11: 61-68
 77. Fox, D. L., Coe, W. R. 1943. Biology of the California sea-mussel (*Mytilus californianus*). *Biol. Bull.* 83: 205-49
 78. Frey-Wyssling, A. 1952. *Deformation and Flow in Biological Systems*. New York: Wiley-Interscience
 79. Gardner, C. R. 1976. The neuronal control of locomotion in the earthworm. *Biol. Rev.* 51: 25-52
 80. Gerber, B. R. 1975. Towards a molecular mechanism for the movement of bacterial flagella: See Ref. 234, Vol. I, pp. 69-87
 81. Gibbons, B. H., Gibbons, I. R. 1972. Flagellar movement and adenosine triphosphate activity in sea urchin sperm extracted with Triton X-100. *J. Cell Biol.* 54: 75-97
 82. Gilboa, A., Silberberg, A. 1975. *In situ* rheological characterization of epithelial mucus. *Biorheology* 13: 59-65
 83. Gittleson, S. M., Hotchkiss, S. K., Valencia, F. G. 1974. Locomotion in the marine dinoflagellate *Amphidinium carterae* (Hulburt). *Trans. Am. Microsc. Soc.* 93: 101-5
 84. Gittleson, S. M., Jahn, T. L. 1968. Flagellar activity of *Polytomella agilis*. *Trans. Am. Microsc. Soc.* 87: 464-71
 85. Gittleson, S. M., Noble, R. M. 1973. Locomotion in *Polytomella agilis* and *Polytoma wella*. *Trans. Am. Microsc. Soc.* 92: 122-28
 86. Gosselin, R. E. 1958. Influence of viscosity on metachronal rhythm of cilia. *Fed. Proc.* 17: 372
 87. Gosselin, R. E. 1966. Physiologic regulators of ciliary motion. *Am. Rev. Respir. Dis.*, 93, no. 3, pt. 2: 41-59
 88. Gosselin, R. E., O'Hara, G. 1961. An unsuspected source of error in studies of particle transport by lamellibranch gill cilia. *J. Cell Comp. Physiol.* 58: 1
 89. Gray, J. 1928. *Ciliary Movement*. Cambridge: Univ. Press. 162 pp.
 90. Gray, J. 1953. Undulatory propulsion. *Q. J. Microsc. Sci.* 94: 551-78

91. Gray, J. 1955. The movement of sea-urchin spermatozoa. *J. Exp. Biol.* 32: 775-801
92. Gray, J. 1968. *Animal Locomotion*. London: Weidenfeld & Nicolson. 479 pp.
93. Gray, J., Hancock, G. J. 1955. The propulsion of sea-urchin spermatozoa. *J. Exp. Biol.* 32: 802-14
94. Graziadei, P. P. C. 1971. Olfactory mucosa of vertebrates. In *Handbook of Sensory Physiology, Vol. IV, pt. 1. Olfaction*, ed. L. M. Beidler, pp. 27-58. Berlin: Springer
95. Halbert, S. A., Tam, P. Y., Blandau, R. J. 1976. Egg transport in the rabbit oviduct: The role of cilia and muscle. *Science* 191: 1052-53
96. Hancock, G. J. 1953. The self-propulsion of microscopic organisms through liquids. *Proc. R. Soc. London Ser. A* 217: 96-121
97. Hand, W. G., Collard, P. A., Davenport, D. 1965. The effects of temperature and salinity change on swimming rate in the dinoflagellates. *Biol. Bull.* 128: 90
98. Hand, W. G., Haupt, W. 1971. Flagellar activity of the colony members of *Volvox aureus* Ehrbg. during light stimulation. *J. Protozool.* 18: 361-64
99. Hand, W. G., Schmidt, J. A. 1975. Phototactic orientation by the marine dinoflagellate *Gyrodinium dorsum* Kofoid. II. Flagellar activity and overall response mechanism. *J. Protozool.* 22: 494-98
100. Harris, J. E. 1961. The mechanics of ciliary movement. In *The Cell and the Organism*, ed. J. A. Ramsay, V. B. Wigglesworth, pp. 22-36. Cambridge: Univ. Press
101. Harris, W. F. 1973. Bacterial flagella, do they rotate or do they propagate waves of bending? *Protoplasma* 77: 477-79
102. Harris, W. F., Robison, W. G. Jr. 1973. Dislocations in microtubular bundles with spermatoxon of the coccid insect *Neosteingelia texana* and evidence for slip. *Nature* 246: 513-15
103. Harvey, C. 1960. The speed of human spermatozoa and the effect on it of various diluents with some preliminary observations on clinical material. *J. Reprod. Fertil.* 1: 84-95
104. Hespell, R. B., Canale-Parola, E. 1970. *Spirochaeta litoralis* sp. n. a strictly anaerobic marine spirochaete. *Arch. Mikrobiol.* 74: 1-18
105. Holwill, M. E. J. 1966a. Physical aspects of flagellar movement. *Physiol. Rev.* 46: 696-785
106. Holwill, M. E. J. 1966b. The motion of *Euglena viridis*: The role of the flagella. *J. Exp. Biol.* 44: 578-88
107. Holwill, M. E. J. 1974. Hydrodynamic aspects of ciliary and flagellar movement. See Ref. 199, pp. 143-76
108. Holwill, M. E. J. 1975. The role of body oscillation in the propulsion of micro-organisms. See Ref. 234, Vol. I, pp. 133-41
109. Holwill, M. E. J., Burge, R. E. 1963. A hydrodynamic study of the motility of flagellated bacteria. *Arch. Biochem. Biophys.* 101: 249-60
110. Holwill, M. E. J., Silvester, N. R. 1965. The thermal dependence of flagellar activity in *Strigomonas oncopeltii*. *J. Exp. Biol.* 42: 537-44
111. Holwill, M. E. J., Sleight, M. A. 1967. Propulsion by hispid flagella. *J. Exp. Biol.* 47: 267-76
112. Hwang, S., Litt, M., Forsman, W. 1969. Rheological properties of mucus. *Rheol. Acta* 8: 438-48
113. Iino, T., Mitani, M. 1966. A mutant of *Salmonella* possessing straight flagella. *J. Gen. Microbiol.* 49: 81-88
114. Jaffrin, M. Y., Shapiro, A. H. 1971. Peristaltic pumping. *Ann. Rev. Fluid Mech.* 3: 13-36
115. Jahn, T. L. 1975. New problems in propulsion of micro-organisms. See Ref. 234, Vol. I, pp. 325-38
116. Jahn, T. L., Bovee, E. C. 1967. Motile behavior of protozoa. In *Research in Protozoology*, ed. T. T. Chen, pp. 41-200. New York: Pergamon
117. Jahn, T. L., Bovee, E. C. 1968. Locomotion of blood protists. In *Infectious Blood Diseases of Man and Animals*, ed. D. Weinman, M. Ristic, pp. 393-436. New York: Academic
118. Jahn, T. L., et al. 1965. Secretory activity of the oral apparatus of ciliates: Trails of adherent particles left by *Paramecium multimicronucleatum* and *Tetrahymena pyriformis*. *Ann. NY Acad. Sci.* 118: 912-20
119. Jahn, T. L., Hendrix, E. M. 1969. Locomotion of the Telotrich ciliate *Opisthnecta henneguyi*. *Rev. Soc. Mex. Hist. Nat.* 30: 103-31
120. Jahn, T. L., Landman, M. D. 1965. Locomotion of spirochetes. *Trans. Am. Microsc. Soc.* 84: 395-406
121. Jahn, T. L., Landman, M. D., Fonseca, J. R. 1964. The mechanism of locomotion in flagellates. II. Function of the mastigonemes of *Ochromonas*. *J. Protozool.* 11: 291-96
122. Jahn, T. L., Votta, J. J. 1972. Loco-

- motion of protozoa. *Ann. Rev. Fluid Mech.* 4: 93-116
123. Kaiser, G. E., Doetsch, R. N. 1975. Enhanced translational motion of *Leptospira* in viscous environments. *Nature* 255: 656-57
 124. Katz, D. F. 1972. *On the biophysics of in vivo sperm transport.* PhD thesis. Univ. Calif., Berkeley. 219 pp.
 125. Katz, D. F. 1974. On the propulsion of micro-organisms near solid boundaries. *J. Fluid Mech.* 64: 33-49
 126. Katz, D. F., Blake, J. R. 1975. Flagellar motions near walls. See Ref. 234, Vol. I, pp. 173-84
 127. Katz, D. F., Blake, J. R., Paveri-Fontana, S. L. 1975. On the movement of slender bodies near plane boundaries at low Reynolds number. *J. Fluid Mech.* 72: 529-40
 128. Keller, S. R., Wu, T. Y. 1976. A porous prolate spheroidal model for ciliated microorganisms. *J. Fluid Mech.* In press
 129. Keller, S. R., Wu, T. Y., Brennen, C. 1975. A traction layer model for ciliary propulsion. See Ref. 234, Vol. I, pp. 253-72
 130. Kensler, C. J., Battista, S. P. 1965. Chemical and physical factors affecting mammalian ciliary activity. *Am. Rev. Respir. Dis.*, 93, no. 3, pt. 2: 93-102
 131. Knight-Jones, E. W. 1954. Relations between metachronism and the direction of ciliary beat in metazoa. *Q. J. Microsc. Sci.* 95(4): 503-21
 132. Koester, H. 1970. Ovum transport. In *Mammalian Reproduction*, ed. H. Gibian, E. J. Plotz, pp. 189-228. New York: Springer
 133. Kudo, R. R. 1954. *Protozoology*. Springfield, Ill.: Thomas. 966 pp.
 134. Landau, L. D. 1944. A new exact solution of the Navier-Stokes equations. *C. R. (Dokl.) Acad. Sci. URSS* 43: 286-88
 135. Lardner, T. J., Shack, W. J. 1972. Cilia transport. *Bull. Math. Biophys.* 34: 325-35
 136. Larsen, S. H., Adler, J., Gargus, J. J., Hogg, R. W. 1974. Chemomechanical coupling without ATP: The source of energy for motility and chemotaxis in bacteria. *Proc. Natl. Acad. Sci. USA* 71: 1239-43
 137. Lee, J. W. 1954. The effect of pH on forward swimming in *Euglena* and *Chilomonas*. *Physiol. Zool.* 27: 272-75
 138. Lehninger, A. L. 1971. *Bioenergetics*. Menlo Park, Calif.: Benjamin. 245 pp.
 139. Leifson, E. 1960. *Atlas of Bacterial Flagellation*. New York: Academic. 171 pp.
 140. Lighthill, M. J. 1952. On the squirming motion of nearly spherical deformable bodies through liquids at very small Reynolds numbers. *Commun. Pure Appl. Math.* 5: 109-18
 141. Lighthill, M. J. 1975. *Mathematical Biofluidynamics*. Philadelphia: SIAM. 281 pp.
 142. Litt, M. 1970. Flow behavior of mucus. *Ann. Otol. Rhinol. Laryngol.* 80: 330-35
 143. Lowndes, A. G. 1944. The swimming of *Monas stigmatica* Pringsheim and *Paramecium trichophorum* (Ehrbg.) Stein and *Volvox* sp. Additional experiments on the working of a flagellum. *Proc. Zool. Soc. London* 114A: 325-38
 144. Lowy, J., Spencer, M. 1968. Structure and function of bacterial flagella. *Symp. Soc. Exp. Biol.* 22: 215-36
 145. Lunec, J. 1975. Fluid flow induced by smooth flagella. See Ref. 234, Vol. I, pp. 143-60
 146. Macherer, H. 1969. Filmbildanalysen 4 verschiedener Schlagmuster der Marginalcirren von *Stylonychia*. *Z. vergl. Physiol.* 62: 183-96
 147. Macherer, H. 1972a. Ciliary activity and the origin of metachrony in *Paramecium*; effects of increased viscosity. *J. Exp. Biol.* 57: 239-60
 148. Macherer, H. 1972b. Temperature influences on ciliary beat and metachronal coordination in *Paramecium*. *J. Mechanochem. Cell Motil.* 1: 97-108
 149. Macherer, H. 1974. Ciliary activity and metachronism in protozoa. See Ref. 199, pp. 199-287
 150. Machin, K. E. 1958. Wave propagation along flagella. *J. Exp. Biol.* 35: 796-806
 151. Macnab, R. M., Koshland, D. E., Jr. 1972. The gradient-sensing mechanism in bacterial chemotaxis. *Proc. Natl. Acad. Sci. USA* 69: 2509-12
 152. Metzner, P. 1920. Die Bewegung und Reizbeantwortung der bipolar begeißelten Spirillen. *Jahrb. Wiss. Bot.* 59: 325-412
 153. Miller, C. E. 1966. Flow induced by mechanical analogues of mucociliary systems. *Ann. NY Acad. Sci.* 130: 880-90
 154. Miller, C. E. 1969. Streamlines, streak lines, and particle path lines associated with a mechanically-induced flow homomorphic with the mammalian mucociliary system. *Biorheology* 6: 127-35
 155. Murakami, A., Takahashi, J. 1975. Correlation of electrical and mechani-

- cal response in nervous control of cilia. *Nature* 257: 48-49
156. Nelson, D. J. 1975. *The distribution, activity and function of the cilia of the brain*. PhD thesis. Univ. Calif., Los Angeles. 196 pp.
 157. Nilsson, O., Reinius, S. 1969. Light and electron microscopic structure of the oviduct. In *The Mammalian Oviduct*, ed. E. S. E. Hafez, R. J. Blandau, pp. 57-83. Chicago: Univ. Chicago Press
 158. Ogiute, K. 1936. Untersuchungen über die Geschwindigkeit der Eigenbewegung von Bakterien. *Jpn. J. Exp. Med.* 14: 19-28
 159. Oscen, C. W. 1927. *Neuere Methoden und Ergebnisse in der Hydrodynamik*. Leipzig: Akad.-Verlag. 337 pp.
 160. Owen, G. 1974. Feeding and digestion in the bivalva. *Adv. Comp. Physiol. Biochem.* 5: 1-36
 161. Parducz, B. 1964. Swimming and its ciliary mechanism in *Ophryoglena* sp. *Acta Protozool.* 2: 367-74 (3 plates)
 162. Parducz, B. 1967. Ciliary movement and coordination in ciliates. *Int. Rev. Cytol.* 21: 91-128
 163. Peters, N. 1929. Über Orts- und Geißelbewegung bei marinen Dinoflagellaten. *Arch. Protistenkd.* 67: 291-321
 164. Phillips, D. M. 1972. Comparative analysis of mammalian sperm motility. *J. Cell Biol.* 53: 561-73
 165. Phillips, D. M. 1974. Structural variants in invertebrate sperm flagella and their relationship to motility. See Ref. 199, pp. 379-402
 166. Prosser, C. L. 1973. *Comparative Animal Physiology*. Vol. II. Philadelphia: Saunders. 554 pp.
 167. Reese, T. S. 1965. Olfactory cilia in the frog. *J. Cell Biol.* 25: 209-30
 168. Reynolds, A. J. 1965. The swimming of minute organisms. *J. Fluid Mech.* 23: 241-60
 169. Rhodin, J. A. G. 1965. Ultrastructure and function of the human tracheal mucosa. *Am. Rev. Respir. Dis.* 93(3): Pt. 2, pp. 1-15
 170. Rikmenspoel, R. 1962. Biophysical approaches to the measurement of sperm motility. In *Spermatozoan Motility*, ed. D. W. Bishop, pp. 31-54. Washington: AAAS
 171. Rikmenspoel, R. 1975. Contraction model for cilia. See Ref. 234, Vol. I, pp. 273-88
 172. Rikmenspoel, R., Sleight, M. A. 1970. Bending moments and elastic constant in cilia. *J. Theor. Biol.* 28: 81-100
 173. Rittenberg, S. 1974. Personal communication
 174. Rivera, J. A. 1962. *Cilia, Ciliated Epithelium and Ciliary Activity*. New York: Pergamon. 167 pp.
 175. Ross, S. M. 1971. *A wavy wall analytic model of muco-ciliary pumping*. PhD thesis. Johns Hopkins Univ., Baltimore, Md. 305 pp.
 176. Ross, S. M., Corrsin, S. 1974. Results of an analytical model of mucociliary pumping. *J. Appl. Physiol.* 37: 333-40
 177. Routledge, L. M. 1975. Bacterial flagella: Structure and function. In *Comparative Physiology—Functional Aspects of Structural Materials*, ed. L. Bolis, H. P. Maddrell, K. Schmidt-Nielsen, pp. 61-73. Amsterdam: North-Holland
 178. Sadé, J., Eliezer, N., Silberberg, A., Nevo, A. C. 1970. The role of mucus in transport by cilia. *Am. Rev. Respir. Dis.* 102: 48-52
 179. Satir, P. 1963. Studies on cilia: I. The fixation of the metachronal wave. *J. Cell Biol.* 18: 345-66
 180. Satir, P. 1965. Studies on cilia: II. Examination of the distal region of the ciliary shaft and the role of the filaments in motility. *J. Cell Biol.* 39: 77-94
 181. Satir, P. 1968. Studies on cilia: III. Further studies on the cilium tip and a "sliding filament" model of ciliary motility. *J. Cell Biol.* 39: 77-94
 182. Satir, P. 1974. The present status of the sliding micro-tubule model of ciliary motion. See Ref. 199, pp. 131-42
 183. Schneider, W. R., Doetsch, R. N. 1974. Effect of viscosity on bacterial motility. *J. Bact.* 117: 696-701
 184. Schreiner, K. E. 1971. The helix as a propeller of microorganisms. *J. Bio-mech.* 4: 73-83
 185. Shack, W. J., Lardner, T. J. 1972. Cilia transport. *Bull. Math. Biophys.* 34: 325-35
 186. Shahar, A., et al 1975. Effect of Δ^9 -tetrahydrocannabinol (THC) on the kinetic morphology of spermatozoa. In *The Functional Anatomy of the Spermatozoon*, ed. B. A. Afzelius, pp. 189-94. New York: Pergamon
 187. Shimada, K., Yoshida, T., Asakura, S. 1975. Cinematographic analysis of the movement of flagellated bacteria. See Ref. 234, Vol. I, pp. 31-43
 188. Shoosmith, J. G. 1960. The measurement of bacterial motility. *J. Gen. Microbiol.* 22: 528-35
 189. Silverman, M., Simon, M. 1974. Flagel-

- lar rotation and the mechanism of bacterial motility. *Nature* 249: 73-74
190. Sleigh, M. A. 1960. The form of beat in cilia of *Stentor* and *Opalina*. *J. Exp. Biol.* 37: 1-10 (1 plate)
 191. Sleigh, M. A. 1962. *The Biology of Cilia and Flagella*. New York: Macmillan. 242 pp.
 192. Sleigh, M. A. 1965. Ciliary coordination in Protozoa. *Progress in Protozoology, 2nd Int. Conf. Protozoology*, Abstr. No. 112, pp. 110-11
 193. Sleigh, M. A. 1966. Some aspects of the comparative physiology of cilia. *Am. Rev. Respir. Dis.* 93: Suppl., pp. 16-31
 194. Sleigh, M. A. 1968. Patterns of ciliary beating. In *Aspects of Cell Motility, Symp. Soc. Exp. Biol.* 22: 131-50
 195. Sleigh, M. A. 1969. Coordination of the rhythm of beat in some ciliary systems. *Int. Rev. Cytol.* 25: 31-54
 196. Sleigh, M. A. 1971. Cilia. *Endeavour* 30: 11-17
 197. Sleigh, M. A. 1972. *Features of ciliary movement of the ctenophores Beroë, Pleurobrachia and Cestus*. In *Essays in Hydrobiology*, ed. R. B. Clark, R. S. Wootton, pp. 119-36. Exeter, Engl.: Univ. Exeter
 198. Sleigh, M. A. 1973. *The Biology of Protozoa*. London: Arnold. 315 pp.
 199. Sleigh, M. A. ed. 1974a. *Cilia and Flagella*. New York: Academic. 500 pp.
 200. Sleigh, M. A. 1974b. Metachronism of cilia of metazoa. See Ref. 199, pp. 287-304
 201. Sleigh, M. A. 1974c. Patterns of movement of cilia and flagella. See Ref. 199, pp. 79-92
 202. Sleigh, M. A. 1976. Fluid propulsion by cilia and physiology of ciliary systems. In *Perspectives in Experimental Biology. Vol. 1, Zoology*, ed. P. S. Davies, pp. 125-34. New York: Pergamon
 203. Sleigh, M. A., Aiello, E. 1972. The movement of water by cilia. *Acta Protozool.* 9: 265-77
 204. Sleigh, M. A., Holwill, M. E. J. 1969. Energetics of ciliary movement in *Sabellaria* and *Mytilus*. *J. Exp. Biol.* 50: 733-44
 205. Slezkin, N. A. 1934. On a case of integrability of the complete differential equations of a viscous fluid. *Moskov. Gos. Univ. Uch. Zap.* 2: 89-90
 206. Smith, J. E., Carthy, J. D., Chapman, G., Clark, R. B., Nichols, D. 1971. *The Invertebrate Panorama*. London: Weidenfeld & Nicolson. 406 pp.
 207. Squire, H. B. 1951. The round laminar jet. *Q. J. Mech. Appl. Math.* 4: 321-29
 208. Stolp, H. 1968. *Bdellovibrio bacteriovorus*—ein räuberischer Bakterienparasit. *Naturwissenschaften* 55: 57-63
 209. Summers, K. E., Gibbons, I. R. 1971. Adenosine triphosphate-induced sliding of tubules in trypsin-treated flagella of sea-urchin sperm. *Proc. Natl. Acad. Sci. USA* 68: 3092-96
 210. Tamm, S. L. 1972. Ciliary motion in *Paramecium*. A scanning electron microscope study. *J. Cell Biol.* 55: 250-55
 211. Tamm, S. L., Horridge, G. A. 1970. The relation between the orientation of the central fibrils and the direction of beat in cilia of *Opalina*. *Proc. R. Soc. London Ser. B* 175: 219-33
 212. Taylor, G. I. 1951. Analysis of the swimming of microscopic organisms. *Proc. R. Soc. London Ser. A* 209: 447-61
 213. Taylor, G. I. 1952a. Analysis of long and narrow animals. *Proc. R. Soc. London Ser. A* 214: 158-83
 214. Taylor, G. I. 1952b. The action of waving cylindrical tails in propelling microscopic organisms. *Proc. R. Soc. London Ser. A* 211: 225-39
 215. Taylor, G. I. 1969. Motion of axisymmetric bodies in viscous fluids. In *Problems of Hydrodynamics and Continuum Mechanics*, pp. 718-24. Philadelphia: SIAM
 216. Tillett, J. P. K. 1970. Axial and transverse Stokes flow past slender axisymmetric bodies. *J. Fluid Mech.* 44: 401-17
 217. Tuck, E. O. 1964. Some methods for flows past slender bodies. *J. Fluid Mech.* 18: 619-35
 218. Tuck, E. O. 1968. A note on a swimming problem. *J. Fluid Mech.* 31: 305-8
 219. Vanderberg, J. P. 1974. Studies on the motility of *Plasmodium* sporozoites. *J. Protozool.* 21: 527-37
 220. van Deurs, B. 1974. Spermatology of some Pycnogonida (Arthropoda), with special reference to a microtubule-nuclear envelope complex. *Acta Zool.* 55: 151-62
 221. Votta, J. J., Jahn, T. L., Griffith, D. L., Fonseca, J. R. 1971. Nature of the flagellar beat in *Trachelomonas volvocina*, *Rhabdomonas spiralis*, *Menoidium cultellus* and *Chilomonas paramecium*. *Trans. Am. Microsc. Soc.* 90: 404-12
 222. Wang, C. Jahn, T. L. 1972. A theory for the locomotion of spirochetes. *J. Theor. Biol.* 36: 53-60
 223. Warner, F. D. 1974. The fine structure

- of the ciliary and flagellar axoneme. See Ref. 199, pp. 11-38
224. Warner, F. D., Satir, P. 1974. The structural basis of ciliary bend formation. Radial spoke positional changes accompanying microtubule sliding. *J. Cell Biol.* 63:35-63
225. Weis-Fogh, T. 1975. Principles of contraction in the spasmoneme of vortice-lids. A new contractile system. In *Comparative Physiology — Functional Aspects of Structural Materials*, ed. L. Bolis, H. P. Maddrell, K. Schmidt-Nielsen, pp. 83-98. Amsterdam: North Holland
226. Weihs, D. 1975. Some hydrodynamic aspects of fish schooling. See Ref. 234, Vol. II, pp. 703-18
227. Williams, M. A., Chapman, G. B. 1961. Electron microscopy of flagellation in species of *Spirillum*. *J. Bact.* 81:195-203
228. Wilson, G. B., et al 1975. Studies on ciliary beating of frog pharyngeal epithelium *in vitro*. II. Relationships between beat form, metachronal coordination, fluid flow and particle transport. See Ref. 234, Vol. I, pp. 301-16
229. Winet, H. 1973. Wall drag on free-moving ciliated microorganisms. *J. Exp. Biol.* 59:753-66
230. Winet, H. 1976. Ciliary propulsion of objects in tubes: Wall drag on swimming *Tetrahymena* (Ciliata) in the presence of mucin and other long-chain polymers. *J. Exp. Biol.* 64:283-302
231. Winet, H., Jahn, T. L. 1974. Geotaxis in protozoa I. A propulsion-gravity model for *Tetrahymena* (Ciliata). *J. Theor. Biol.* 46:449-65
232. Winet, H., Jones, A. R. 1975. Mucocysts in spirostomum (ciliata: heterotricha). *J. Protozool.* 22:293-96
233. Winet, H., Keller, S. R. 1976. Spirillum swimming. Theory and observations of propulsion by the flagellar bundle. *J. Exp. Biol.* In press
234. Wu, T. Y., Brokaw, C. J., Brennen, C., eds. 1975. *Swimming and Flying in Nature*, Vols. 1, 2. New York: Plenum. 1005 pp.
235. Yoneda, M. 1962. Force exerted by a single cilium of *Mytilus edulis* II. Free motion. *J. Exp. Biol.* 39:307-17